Pergamon

Int. J. Solids Structures Vol. 35, No. 18, pp. 2315–2347, 1998

0020-7683/98 $19.00 + .00

PII: S0020-7683(97)00184-4

A MODEL FOR THE NONLINEAR VISCOELASTIC RESPONSE IN POLYMERS AT FINITE STRAINS

ALEKSEY D. DROZDOV
Institute for Industrial Mathematics, Ben-Gurion University of the Negev, 22 Ha-Histadrut Street, Be'ersheba, 84213 Israel

(*Received* 12 *December* 1996; *in revised form* 18 *June* 1997)

Abstract—New constitutive equations are derived for viscoelastic media which do not possess the separability property. The model extends the concept of transient polymeric networks by assuming the rates of breakage and reformation of adaptive links to depend on strain energy density. This permits mechanically induced aging/rejuvenation of polymers to be described.

To verify the constitutive relations, we use experimental data obtained in tensile relaxation tests for poly(methyl methacrylate) and polycarbonate, in shear relaxation tests for poly(methyl methacrylate) and an epoxy glass, and in tensile tests with constant rate of strains for ethylene–butene and ethylene–octene copolymers, poly(ethylene terephthalate), and polycarbonate at strains up to 300 per cent. The model provides fair agreement between observations and their predictions.

As an example of inhomogeneous deformations, we analyze inflation of a thick-walled viscoelastic spherical vessel under the action of internal pressure. The effect of material parameters on stresses and displacements is studied numerically. © 1998 Elsevier Science Ltd. All rights reserved.

1. INTRODUCTION

The paper is concerned with constitutive relations for the nonlinear viscoelastic behavior of polymers under isothermal loading at finite strains.

Constitutive models in finite viscoelasticity have attracted essential attention in the past three decades due to their applications in polymer engineering. However, a majority of the studies have dealt with viscoelastic media obeying the separability principle, which implies that the effects of time and strains on the mechanical response may be separated (to a certain extent).

As common practice, the separability property is demonstrated in one-step relaxation tests, where the stress is factorized into the product of a function of time (the relaxation modulus in linear viscoelasticity) and a function of strains (the damping function), see, e.g. Wagner (1976). This implies that the relaxation curves obtained at different strain levels and plotted in the bi-logarithmic coordinates are parallel to each other. Experimental evidence of the separability property is produced by Bloch *et al.* (1978) and Glucklich and Landel (1977) for styrene-butadiene rubber, by Isono and Ferry (1985) and Titomanlio (1980) for polyisobutylene, by Khan *et al.* (1987) and Laun (1978) for polyethylene, and by Soskey and Winter (1985) for polyethylene and polystyrene. However, even in those studies some deviations are observed from the separability principle at large strains (about 100 per cent), see, e.g. Soskey and Winter (1985), and at large times (about 15 min), see, e.g. Titomanlio *et al.* (1980). Moreover, prediction of the response in two-steps relaxation tests based on the separability hypothesis leads to serious discrepancies between experimental data and results of numerical simulation, see, e.g. Petruccione and Biller (1988) and Titomanlio *et al.* (1980).

Non-parallelness of relaxation curves measured at different strain levels have been demonstrated by Litt and Torp (1973), Ricco and Smith (1985), Tervoort *et al.* (1996), and Yee *et al.* (1988) for polycarbonate, by McKenna and Zapas (1979) and Marrucci and de Cindio (1980) for poly(methyl methacrylate), and by Santore *et al.* (1991) and Waldron *et al.* (1995) for an epoxy glass. In the framework of the K-BKZ theory, this phenomenon may be explained by the effect of strains on some "internal clock", and it is referred to as the mechanically induced rejuvenation of polymers (e.g. Struik, 1978; Waldron *et al.*, 1995; and the bibliography therein).

The idea of reduced (or internal) time for the prediction of the nonlinear viscoelastic response goes back to Leaderman (1943), who proposed to replace the absolute time t in the integral constitutive equations by some internal time ξ to account for the effect of strains on the current stress. At infinitesimal strains, the internal time coincides with the absolute time, while at large deformations, the internal time is determined by the formula

$$\xi(t) = \int_0^t \frac{d\tau}{a(\tau)}, \tag{1}$$

where the shift factor $a(t)$ is a function of the current strain tensor $\boldsymbol{\varepsilon}(t)$.

Equation (1) imposes strong restrictions on the relaxation spectrum, since it implies that the relaxation times T_m change similarly to each other

$$\frac{T_m(\boldsymbol{\varepsilon})}{T_m(0)} = a(\boldsymbol{\varepsilon}). \tag{2}$$

Formula (2) has been questioned by several authors (e.g. McCrum, 1984). In particular, using experimental data for poly(methyl methacrylate), Read (1981) demonstrated that the ratio in the left-hand side of eqn (2) increases with the growth of m.

The main disadvantage of the concept of internal time is that no physical model exists to describe the effect of strains on the shift function a. Schapery (1966) suggested to treat a as an adjustable function which is found by fitting experimental data. La Mantia (1977) and La Mantia and Titomanlio (1979) assumed that the shift function a was connected with the fractional free volume f by the Doolittle equation (Doolittle, 1951),

$$\ln a = B\left(\frac{1}{f} - \frac{1}{f_0}\right), \tag{3}$$

where f is the free volume fraction at the strain $\boldsymbol{\varepsilon}$, f_0 is the free volume fraction at the zero strain, and B is an adjustable parameter.

Formally, eqn (3) does not simplify the problem, since it expresses one unknown function a in terms of another unknown function f. As common practice, the free volume fraction f is assumed to change linearly with volume deformation (e.g. La Mantia, 1977; Knauss and Emri, 1981; Shay and Caruthers, 1986; Losi and Knauss, 1992; Chengalva *et al.*, 1995). According to more sophisticated models, f satisfies a linear differential equation, the right-hand side of which depends linearly on the volume deformation (e.g. La Mantia and Titomanlio, 1979). Knauss and Emri (1987) proposed to replace the differential equation for the function f by a linear integral equation.

The above models predict the effect of dilatation on the relaxation spectrum. To account for the influence of shear strains [this effect was confirmed experimentally by McKenna and Zapas (1979)], Wineman and Waldron (1993, 1995) supposed that the free volume fraction increased linearly with the growth of the local shear, see also Waldron *et al.* (1995) and the bibliography therein.

A linear dependence of the free volume fraction on the shear strain allows two physical phenomena to be described in the framework of the nonlinear viscoelasticity: (i) the effect of strains on relaxation spectra; and (ii) the yield-like behavior of polymers under tension (a local maximum on the stress–strain diagram $\sigma(\varepsilon)$, a decreasing branch of the $\sigma(\varepsilon)$ curve immediately after the yield point, and an increasing branch of this curve at large strains). As serious drawbacks of this approach, we may mention (i) the absence of experimental verification for basic postulates, and (ii) the absence of a physical concept which permits phenomenological equations to be interpreted at the micro-level.

The objective of the present paper is to derive a model for nonlinear viscoelastic media with some "internal clock" based on the concept of transient polymeric networks (e.g. Green and Tobolsky, 1946; Yamamoto, 1956; Lodge, 1968; Tanaka and Edwards, 1992).

According to that concept, a polymeric material is thought of as a network of adaptive links (springs) which break and emerge. The links model chemical and physical crosslinks, as well as entanglements between polymeric chains. Using the balance law for the number of links, we derive partial differential equations for the breakage functions. Coefficients of these equations (the reformation rates) are constant for the linear viscoelastic behavior. Assuming these coefficients to depend on strain energy density of adaptive links, we arrive at new constitutive equations in the nonlinear viscoelasticity.

According to basic axioms of the constitutive theory (e.g. Truesdell, 1975), the stress tensor at the current instant t is entirely determined by the deformation history up to the instant t. Relationships presenting the stress as a tensor-valued functional on strain histories may be referred to as explicit constitutive equations. It is worth also mentioning constitutive models with the so-called "stress-induced internal clock" (stress-dependent relaxation spectra), which determine the stress implicitly as a functional on both strain and stress histories (e.g. Kaye, 1966; Bernstein and Shokooh, 1980; Tervoort *et al.*, 1996).

The question of what is the real reason for changes in the characteristic times of relaxation remains open up to date. In the present work, we confine ourselves to "explicit" integral constitutive equations with a strain-induced internal clock. However, the energy approach (which implies that a strain energy density determines reformation of adaptive links) allows us to account for effects of both mechanical factors on the relaxation spectrum. To derive a model with a "strain clock", it suffices to assume that the strain energy density is a function of strains, while to arrive at a constitutive model with a "stress clock", we assume that the strain energy density is a function of stresses.

The paper is organized as follows. Section 2 is concerned with a model of adaptive links. We derive some presentation for the relaxation kernel of a non-aging linear viscoelastic medium and extend the governing equations to viscoelastic media with strain-dependent relaxation spectra. In Section 3, we discuss the time–strains superposition principle and propose a new phenomenological equation for the shift factor. Constitutive equations for viscoelastic materials which do not possess the separability property are developed in Section 4. As a particular case, we consider constitutive relations for a neo-Hookean viscoelastic medium with a strain-dependent spectrum. Uniaxial tension of a viscoelastic specimen is studied in Section 5, and simple shear is analyzed in Section 6. Explicit solutions are derived for nonlinear, incompressible, viscoelastic media with finite strains, and the obtained relations are verified by comparison with experimental data for several polymers. Section 7 deals with inflation of a viscoelastic hollow sphere at large deformations. Some concluding remarks are formulated in Section 8.

2 A MODEL OF ADAPTIVE LINKS

According to the concept of transient polymeric networks, a viscoelastic medium is modeled as a system of parallel elastic springs (links between polymeric chains) which break and arise. It is assumed that $\bar{X}_0$ initial links are not involved in the reformation process, and M different kinds of replacing links exist which correspond to M different characteristic times of relaxation (e.g., He and Song, 1993). The number of links of the mth kind arisen before instant τ and existing at instant t is denoted as $X_m(t, \tau)$. The quantities $\bar{X}_0$ and $X_m(t, \tau)$ determine the numbers of adaptive links per unit volume in the reference configuration.

The function $X_m(t, \tau)$ entirely characterizes breakage of existing links and creation of new links of the mth kind. For example, the derivative

$$\frac{\partial X_m}{\partial t}(t, \tau)$$

equals the rate of annihilation (at the current instant t) for adaptive links emerged before instant τ, while the derivative

$$\frac{\partial X_m}{\partial \tau}(t,\tau)$$

equals the rate of creation of new links (at instant τ) which survive until the current instant t.

We introduce the relative rates of reformation

$$\gamma_m(\tau) = \frac{1}{\bar{X}_m}\frac{\partial X_m}{\partial \tau}(t,\tau)|_{t=\tau}, \tag{4}$$

where $\bar{X}_m = X_m(0,0)$, and the breakage functions $g_m(t,\tau)$. The quantity $g_m(t,\tau)$ equals the relative number of adaptive links of the mth kind existed at instant τ and broken to instant t. Evidently,

$$\begin{aligned} X_m(t,0) &= X_m(0,0)[1-g_m(t,0)] = \bar{X}_m[1-g_m(t,0)], \\ \frac{\partial X_m}{\partial \tau}(t,\tau) &= \frac{\partial X_m}{\partial \tau}(t,\tau)|_{t=\tau}[1-g_m(t,\tau)] = \bar{X}_m\gamma_m(\tau)[1-g_m(t,\tau)]. \end{aligned} \tag{5}$$

Substitution of expressions (4) and (5) into the formula

$$X_m(t,t) = X_m(t,0) + \int_0^t \frac{\partial X_m}{\partial \tau}(t,\tau)\,d\tau$$

yields

$$X_m(t,t) = \bar{X}_m\left\{1-g_m(t,0) + \int_0^t \gamma_m(\tau)[1-g_m(t,\tau)]\,d\tau\right\}. \tag{6}$$

We begin with the analysis of the balance eqn (6) for non-aging viscoelastic media, the mechanical properties of which are independent of time. For non-aging materials,

$$X_m(t,t) = \bar{X}_m, \quad \gamma_m(t) = \gamma_{m0}, \quad g_m(t,\tau) = g_{m0}(t-\tau), \tag{7}$$

which mean that the total number of links remains unchanged, the rate of reformation is time-independent, and the relative number of adaptive links arisen before instant τ and broken to instant t is determined by the difference $t-\tau$ only. It follows from eqns (6) and (7) that

$$g_{m0}(t) = \gamma_{m0}\int_0^t [1-g_{m0}(\tau)]\,d\tau.$$

Differentiation of this equality implies that

$$\frac{dg_{m0}}{dt}(t) = \gamma_{m0}[1-g_{m0}(t)], \quad g_{m0}(0) = 0. \tag{8}$$

Solving eqn (8), we find that

$$g_{m0}(t) = 1-\exp(-\gamma_{m0}t). \tag{9}$$

We substitute expression (9) into eqn (5), use eqn (7), and obtain

$$X_m(t,0) = \bar{X}_m \exp(-\gamma_{m0} t), \quad \frac{\partial X_m}{\partial \tau}(t,\tau) = \bar{X}_m \gamma_{m0} \exp[-\gamma_{m0}(t-\tau)]. \tag{10}$$

It follows from eqns (7) and (10) and the formula

$$X_m(t,\tau) = X_m(t,t) - \int_\tau^t \frac{\partial X_m}{\partial s}(t,s)\,\mathrm{d}s,$$

that the total number of adaptive links (per unit volume) arisen before instant τ and existing at instant t

$$X(t,\tau) = \bar{X}_0 + \sum_{m=1}^{M} X_m(t,\tau) \tag{11}$$

is calculated as

$$\begin{aligned} X(t,\tau) &= \bar{X}_0 + \sum_{m=1}^{M} \bar{X}_m \exp[-\gamma_{m0}(t-\tau)] \\ &= \bar{X}\left\{\eta_0 + \sum_{m=1}^{M} \eta_m \exp[-\gamma_{m0}(t-\tau)]\right\}, \end{aligned} \tag{12}$$

where

$$\bar{X} = \sum_{m=0}^{M} \bar{X}_m, \quad \eta_m = \frac{\bar{X}_m}{\bar{X}}. \tag{13}$$

In linear viscoelasticity, the function $X(t,\tau)$ coincides with the relaxation kernel of a viscoelastic medium (e.g. Drozdov, 1996). According to eqn (12), the relaxation kernel of an arbitrary non-aging viscoelastic material can be presented in the form of a truncated Prony series.

To describe the mechanical meaning of eqn (8), we consider a subsystem of the system of adaptive links of the mth kind, which contains $v_m(\tau)$ links at instant τ. By analogy with eqn (5), the number of links $v_m(t)$ in this subsystem at an arbitrary instant t is calculated as

$$v_m(t) = v_m(\tau)[1 - g_m(t,\tau)]. \tag{14}$$

Differentiation of eqn (14) with the use of eqns (7) and (8) implies that

$$\begin{aligned} \frac{\mathrm{d}v_m}{\mathrm{d}t}(t) &= -v_m(\tau)\frac{\partial g_m}{\partial t}(t,\tau) = -v_m(\tau)\frac{\mathrm{d}g_{m0}}{\mathrm{d}t}(t-\tau) \\ &= -\gamma_{m0} v_m(\tau)[1 - g_{m0}(t-\tau)] = -\gamma_{m0} v_m(\tau)[1 - g_m(t,\tau)] \\ &= -\gamma_{m0} v_m(t). \end{aligned} \tag{15}$$

According to eqn (15), formula (8) means that for any subsystem of the system of adaptive links of the mth kind, the relative rate of breakage equals γ_{m0}

$$\frac{1}{v_m(t)}\frac{\mathrm{d}v_m}{\mathrm{d}t}(t) = -\gamma_{m0}. \tag{16}$$

In viscoelastic materials with strain-dependent spectra, eqns (7) do not hold. For an arbitrary loading history, the rates of reformation γ_m depend explicitly on time, while the

breakage functions g_m depend on two separate variables t and τ (as a consequence of dependencies of γ_m and g_m on strains, which, in turn, change in time). The latter may be thought of as an apparent aging/rejuvenation of polymers (Ricco and Smith, 1985; Waldron *et al.*, 1995).

For aging materials, the balance eqn (6) can help a little, because it contains three unknown functions $X_m(t, t)$, $\gamma_m(t)$, and $g_m(t, \tau)$. Our analysis of the response in aging viscoelastic media is based on the following two hypotheses:

- the relative rates of reformation $\gamma_m(t)$ are prescribed functions of time;
- formula (16) is satisfied both for non-aging and aging polymers. In the latter case it reads

$$\frac{\partial g_m}{\partial t}(t,\tau) = \gamma_m(t)[1-g_m(t,\tau)], \quad g_m(\tau,\tau) = 0. \tag{17}$$

A phenomenological relationship similar to eqn (17) has been proposed by Petruccione and Biller (1988). The difference between the two models consists in the following: according to our approach, eqn (17) determines entirely the reforation process, while in the Petruccione–Biller model an additional formula is necessary for the reformation rate.

It follows from eqns (5) and (17) that the functions

$$n_m(t) = \frac{X_m(t,0)}{\bar{X}_m}, \quad N_m(t,\tau) = \frac{1}{\bar{X}_m}\frac{\partial X_m}{\partial \tau}(t,\tau) \tag{18}$$

are governed by the differential equations

$$\frac{1}{n_m(t)}\frac{\mathrm{d}n_m}{\mathrm{d}t}(t) = -\gamma_m(t), \quad n_m(0) = 1,$$

$$\frac{1}{N_m(t,\tau)}\frac{\partial N_m}{\partial t}(t,\tau) = -\gamma_m(t), \quad N_m(\tau,\tau) = \gamma_m(\tau). \tag{19}$$

Given functions $\gamma_m(t)$, eqn (19) determines the numbers of links of the mth kind which exist at time t.

3. TIME–STRAINS SUPERPOSITION PRINCIPLE

To derive expressions for the reformation rates γ_m, we return to eqn (2) and suppose that the relaxation times T_m change similarly to each other. Formula (2) is confirmed by experimental data for a number of polymers at different temperatures and pressure levels (Ferry, 1980). As common practice, eqn (2) is used for the analysis of data obtained in static and dynamic tests at various absolute temperatures ϑ and it is referred to as the time–temperature superposition principle, while the function $a = a(\vartheta)$ is the thermal shift factor.

The effect of temperature on the relaxation times may be described by the Doolittle equation

$$\ln a(\vartheta) = \ln\frac{T_m(\vartheta)}{T_m(\vartheta_0)} = \frac{\Delta}{R}\left(\frac{1}{f}-\frac{1}{f_0}\right), \tag{20}$$

where Δ is an activation enthalpy and R is the Boltzmann constant. By assuming the function f in eqn (20) to depend linearly on the temperature ϑ,

$$f = f_0 + \alpha_\vartheta(\vartheta-\vartheta_0), \tag{21}$$

where α_ϑ is a coefficient of thermal expansion, we arrive at the WLF-equation (Ferry, 1980),

which correctly predicts the effect of temperature on the relaxation spectrum for a number of polymers (mainly, above the glass transition temperature).

To describe the effect of dilatation on the relaxation times, Knauss and Emri (1981, 1987) suggested to add a term proportional to the volume deformation to the right-hand side of eqn (21). This model has been verified using experimental data for poly(vinyl acetate), see Knauss and Emri (1987), and polyethylene, see Chengalva *et al.* (1995). By analogy with that approach, Wineman and Waldron (1993, 1995) suggested to add two terms to the right-hand side of eqn (21). The first one is proportional to dilatation, while the other is proportional to the shear deformation. To the best of our knowledge, that model has not yet been verified by comparison with experimental data.

We confine ourselves to isothermal loading and propose the following formula for the free volume fraction similar to that suggested by Knauss and Emri (1981, 1987) and Wineman and Waldron (1993, 1995):

$$f = f_0 + \tilde{\beta}\tilde{W}_0. \tag{22}$$

Here $\tilde{W}_0$ is some strain energy density, and $\tilde{\beta}$ is an adjustable parameter.

Equation (22) may be treated as a truncated Taylor series for the function $f(\tilde{W}_0)$ where terms of the second order are neglected. The latter means that eqn (22) should be satisfied at least when the function $f(\tilde{W}_0)$ is sufficiently smooth and the mechanical energy $\tilde{W}_0$ is small. We will demonstrate later that eqn (22) is in fair agreement with experimental data for a number of polymeric materials at strains up to 300 per cent.

Combining eqns (20) and (22), we obtain

$$\ln a = \frac{\Delta}{R}\left(\frac{1}{f_0 + \tilde{\beta}\tilde{W}_0} - \frac{1}{f_0}\right) = B\left(\frac{1}{1+\beta\tilde{W}_0} - 1\right), \tag{23}$$

where

$$B = \frac{\Delta}{Rf_0}, \quad \beta = \frac{\tilde{\beta}}{f_0}.$$

To analyze experimental data, we employ the ratio

$$a_0(\boldsymbol{\varepsilon}) = \frac{T_m(\boldsymbol{\varepsilon})}{T_m(\boldsymbol{\varepsilon}_0)} \tag{24}$$

instead of the shift function $a(\boldsymbol{\varepsilon})$, see eqn (2). Here $\boldsymbol{\varepsilon}_0$ is a given strain tensor. It follows from eqns (23) and (24) that

$$\ln a_0(\boldsymbol{\varepsilon}) = \ln\frac{T_m(\boldsymbol{\varepsilon})}{T_m(0)} + \ln\frac{T_m(0)}{T_m(\boldsymbol{\varepsilon}_0)} = B\left(\frac{1}{1+\beta\tilde{W}_0} - 1\right) + B_0, \tag{25}$$

where

$$B_0 = \ln\frac{T_m(0)}{T_m(\boldsymbol{\varepsilon}_0)}.$$

Since the reformation rates γ_m are inversely proportional to the characteristic times of relaxation,

$$\gamma_m = T_m^{-1}, \tag{26}$$

equation (25) implies that for any m,

$$\gamma_m(\varepsilon) = \frac{\gamma_m(\varepsilon_0)}{a_0(\varepsilon)} = \gamma_m(\varepsilon_0)\exp\left\{-\left[B_0 + B\left(\frac{1}{1+\beta\tilde{W}_0} - 1\right)\right]\right\}. \tag{27}$$

Given strain history $\varepsilon(t)$ and strain energy density $\tilde{W}_0(\varepsilon)$, eqns (19) and (27) determine entirely breakage and reformation of adaptive links.

There are several approaches to define the function $\tilde{W}_0$ in eqn (23). For example, we may assume that $\tilde{W}_0$ equals the strain energy density (per unit volume) of a viscoelastic material. In that case, the mechanical energy of all existing links determines the reformation process.

Another way is to suppose that reformation of any kind of adaptive links is determined by its own energy density. The latter implies that similarity of the relaxation times T_m fails in accordance with Read (1981).

We may assume that there is some "basic" kind of links, whose strain energy density determines the rates of reformation for other kinds of adaptive links. Buckley and Jones (1995) distinguished two types of chemical links: strong (which characterize bond stretching), and weak (which characterize changes of molecular conformations) and supposed that only strong links were responsible for anelastic processes in polymers. Treating nonreplacing links as an analog of strong bonds, we assume that their strain energy density $\tilde{W}_0$ determine the breakage and reformation processes.

Equation (23) provides a simple physical model for the analysis of transient networks. However, formula (23) should be considered rather as a phenomenological equation to be confirmed by observations than a physical law for interactions between polymeric molecules. Validation of this equation by comparison of numerical results with experimental data will be carried out in Sections 5 and 6.

4. CONSTITUTIVE EQUATIONS FOR A VISCOELASTIC MEDIUM

An adaptive link of the mth kind is modeled as an incompressible, isotropic, hyperelastic solid, the potential energy W_m of which depends on the first invariants I_1 and I_2 of some Finger tensor $\mathbf{F}$. We assume that the natural (stress-free) state of a link which merges with the network at instant τ coincides with the actual configuration of the system. This means that we can set

$$\mathbf{F} = \mathbf{F}^0(t)$$

for the initial links (existed at $t = 0$) and set

$$\mathbf{F} = \mathbf{F}^\circ(t,\tau)$$

for links arisen at instant τ. Here $\mathbf{F}^0(t)$ is the Finger tensor for transition from the initial to the actual configuration, and $\mathbf{F}^\circ(t,\tau)$ is the relative Finger tensor for transition from the actual configuration at instant τ to the actual configuration at instant t.

Summing up potential energies for adaptive links existing at instant t, we obtain the total potential energy of the system

$$\bar{W}(t) = \bar{X}_0 W_0(I_k(\mathbf{F}^0(t))) + \sum_{m=1}^{M}\left[X_m(t,0)W_m(I_k(\mathbf{F}^0(t))) + \int_0^t \frac{\partial X_m}{\partial\tau}(t,\tau)W_m(I_k(\mathbf{F}^\circ(t,\tau)))\,d\tau\right]. \tag{28}$$

Substitution of expressions (13) and (18) into eqn (28) implies that

$$\bar{W}(t) = \eta_0 \tilde{W}_0(I_k(\mathbf{F}^0(t))) + \sum_{m=1}^{M} \eta_m \left[n_m(t) \tilde{W}_m(I_k(\mathbf{F}^0(t))) + \int_0^t N_m(t,\tau) \tilde{W}_m(I_k(\mathbf{F}^\circ(t,\tau)))\, \mathrm{d}\tau \right], \quad (29)$$

where

$$\tilde{W}_m = W_m \bar{X}. \quad (30)$$

There are two ways to derive the stress–strain relations for an incompressible viscoelastic medium with a given strain energy density per unit volume $\bar{W}(t)$. According to the first, the Lagrange variational principle is employed to obtain an explicit formula for the Cauchy stress tensor $\boldsymbol{\sigma}(t)$ (e.g. Drozdov, 1993). According to the other technique, the stress tensor is calculated using an analog of the Finger formula for a viscoelastic material (e.g. Drozdov, 1996). Both approaches entail the constitutive equation (simple, but tedious calculations are omitted)

$$\boldsymbol{\sigma}(t) = -p(t)\mathbf{I} + 2\left\{ \eta_0 \boldsymbol{\Theta}_0(t) + \sum_{m=1}^{M} \eta_m \left[n_m(t) \boldsymbol{\Theta}_m(t) + \int_0^t N_m(t,\tau) \boldsymbol{\Theta}_m^\circ(t,\tau)\, \mathrm{d}\tau \right] \right\}. \quad (31)$$

Here p is pressure, $\mathbf{I}$ is the unit tensor, and

$$\boldsymbol{\Theta}_m(t) = \sum_{k=1}^{2} \Psi_{m,k}(t)[\mathbf{F}^0(t)]^k, \quad \boldsymbol{\Theta}_m^\circ(t,\tau) = \sum_{k=1}^{2} \Psi_{m,k}^\circ(t,\tau)[\mathbf{F}^\circ(t,\tau)]^k, \quad (32)$$

where

$$\Psi_{m,1}(t) = \frac{\partial \tilde{W}_m}{\partial I_1}(I_k^0(t)) + I_1^0(t) \frac{\partial \tilde{W}_m}{\partial I_2}(I_k^0(t)),$$

$$\Psi_{m,2}(t) = -\frac{\partial \tilde{W}_m}{\partial I_2}(I_k^0(t)),$$

$$\Psi_{m,1}^\circ(t,\tau) = \frac{\partial \tilde{W}_m}{\partial I_1}(I_k^\circ(t,\tau)) + I_1^\circ(t,\tau) \frac{\partial \tilde{W}_m}{\partial I_2}(I_k^\circ(t,\tau)),$$

$$\Psi_{m,2}^\circ(t,\tau) = -\frac{\partial \tilde{W}_m}{\partial I_2}(I_k^\circ(t,\tau)),$$

$$I_k^0(t) = I_k(\mathbf{F}^0(t)), \quad I_k^\circ(t,\tau) = I_k(\mathbf{F}^\circ(t,\tau)). \quad (33)$$

Given strain energy densities $W_m(I_1, I_2)$ $(m = 0, 1, \ldots, M)$, integro-differential eqns (19), (27), and (31) to (33) determine the response in a viscoelastic medium which does not obey the separability principle.

As a particular case, we assume that all kinds of adaptive links are governed by the constitutive equations of a neo-Hookean elastic solid with the strain energy density

$$\tilde{W}_m = \frac{\mu_m}{2}(I_1 - 3), \quad (34)$$

where μ_m is the generalized elastic modulus. Substitution of expression (34) into eqns (32) and (33) implies that

$$\Psi_{m,1}(t) = \Psi^{\circ}_{m,1}(t,\tau) = \frac{\mu_m}{2}, \quad \Psi_{m,2}(t) = \Psi^{\circ}_{m,2}(t,\tau) = 0,$$

$$\mathbf{\Theta}_m(t) = \frac{\mu_m}{2}\mathbf{F}^0(t), \quad \mathbf{\Theta}^{\circ}_m(t,\tau) = \frac{\mu_m}{2}\mathbf{F}^{\circ}(t,\tau).$$

Combining these equalities with eqn (31), we arrive at the formula

$$\boldsymbol{\sigma}(t) = -p(t)\mathbf{I} + \mu_0\eta_0\mathbf{F}^0(t) + \sum_{m=1}^{M}\mu_m\eta_m\left[n_m(t)\mathbf{F}^0(t) + \int_0^t N_m(t,\tau)\mathbf{F}^{\circ}(t,\tau)\,d\tau\right]. \tag{35}$$

Bearing in mind that

$$\eta_0 = 1 - \sum_{m=1}^{M}\eta_m,$$

we present eqn (35) as follows:

$$\boldsymbol{\sigma}(t) = -p(t)\mathbf{I} + \left[\mu_0 - \sum_{m=1}^{M}\eta_m(\mu_0 - \mu_m n_m(t))\right]\mathbf{F}^0(t) + \sum_{m=1}^{M}\mu_m\eta_m\int_0^t N_m(t,\tau)\mathbf{F}^{\circ}(t,\tau)\,d\tau. \tag{36}$$

Formula (36) provides the constitutive equation for a neo-Hookean viscoelastic medium with a strain-dependent relaxation spectrum, where the functions $n_m(t)$ and $N_m(t,\tau)$ satisfy eqn (19), while the rates of reformation of adaptive links γ_m are calculated according to eqn (27).

5. UNIAXIAL TENSION OF A SPECIMEN

To analyze the constitutive model eqns (19), (27), and (31), we consider uniaxial tension of a specimen

$$x^1 = \lambda(t)X^1, \quad x^2 = \lambda_0(t)X^2, \quad x^3 = \lambda_0(t)X^3, \tag{37}$$

where X^i and x^i are Cartesian coordinates in the initial and actual configuration. It follows from eqn (37) that the deformation gradient $\vec{\nabla}_0\bar{r}(t)$ equals

$$\vec{\nabla}_0\bar{r}(t) = \lambda(t)\bar{\mathbf{e}}_1\bar{\mathbf{e}}_1 + \lambda_0(t)(\bar{\mathbf{e}}_2\bar{\mathbf{e}}_2 + \bar{\mathbf{e}}_3\bar{\mathbf{e}}_3), \tag{38}$$

where $\bar{\mathbf{e}}_i$ are unit vectors of the Cartesian coordinate frame in the initial configuration. Equation (38) implies that the Finger tensors $\mathbf{F}^0(t)$ and $\mathbf{F}^{\circ}(t,\tau)$ are calculated as

$$\mathbf{F}^0(t) = \lambda^2(t)\bar{\mathbf{e}}_1\bar{\mathbf{e}}_1 + \lambda_0^2(t)(\bar{\mathbf{e}}_2\bar{\mathbf{e}}_2 + \bar{\mathbf{e}}_3\bar{\mathbf{e}}_3),$$

$$\mathbf{F}^{\circ}(t,\tau) = \left(\frac{\lambda(t)}{\lambda(\tau)}\right)^2\bar{\mathbf{e}}_1\bar{\mathbf{e}}_1 + \left(\frac{\lambda_0(t)}{\lambda_0(\tau)}\right)^2(\bar{\mathbf{e}}_2\bar{\mathbf{e}}_2 + \bar{\mathbf{e}}_3\bar{\mathbf{e}}_3). \tag{39}$$

It follows from eqn (39) and the incompressibility condition

$$I_3^0(t) = 1 \tag{40}$$

that

$$\lambda_0(t) = \lambda^{-1/2}(t). \tag{41}$$

We substitute expression (41) into eqn (39) and find that

$$\begin{aligned}
\mathbf{F}^0(t) &= \lambda^2(t)\bar{\mathbf{e}}_1\bar{\mathbf{e}}_1 + \lambda^{-1}(t)(\bar{\mathbf{e}}_2\bar{\mathbf{e}}_2 + \bar{\mathbf{e}}_3\bar{\mathbf{e}}_3),\\
\mathbf{F}^\diamond(t,\tau) &= \left(\frac{\lambda(t)}{\lambda(\tau)}\right)^2 \bar{\mathbf{e}}_1\bar{\mathbf{e}}_1 + \frac{\lambda(\tau)}{\lambda(t)}(\bar{\mathbf{e}}_2\bar{\mathbf{e}}_2 + \bar{\mathbf{e}}_3\bar{\mathbf{e}}_3),\\
I_1^0(t) &= \lambda^2(t) + 2\lambda^{-1}(t), \quad I_2^0(t) = 2\lambda(t) + \lambda^{-2}(t),\\
I_1^\diamond(t,\tau) &= \left(\frac{\lambda(t)}{\lambda(\tau)}\right)^2 + 2\frac{\lambda(\tau)}{\lambda(t)}, \quad I_2^\diamond(t,\tau) = 2\frac{\lambda(t)}{\lambda(\tau)} + \left(\frac{\lambda(\tau)}{\lambda(t)}\right)^2.
\end{aligned} \tag{42}$$

Combining expressions (31), (32), and (42), we obtain

$$\boldsymbol{\sigma}(t) = \sigma_1(t)\bar{\mathbf{e}}_1\bar{\mathbf{e}}_1 + \sigma_2(t)\bar{\mathbf{e}}_2\bar{\mathbf{e}}_2 + \sigma_3(t)\bar{\mathbf{e}}_3\bar{\mathbf{e}}_3, \tag{43}$$

where

$$\begin{aligned}
\sigma_1(t) = {} & -p(t) + 2\lambda^2(t)\left\{\eta_0\Psi_{0,1}(t) + \sum_{m=1}^{M}\eta_m[n_m(t)\Psi_{m,1}(t) + Y_{m,1,-2}(t)]\right\}\\
& + 2\lambda^4(t)\left\{\eta_0\Psi_{0,2}(t) + \sum_{m=1}^{M}\eta_m[n_m(t)\Psi_{m,2}(t) + Y_{m,2,-4}(t)]\right\},\\
\sigma_2(t) = \sigma_3(t) = {} & -p(t) + 2\lambda^{-1}(t)\left\{\eta_0\Psi_{0,1}(t) + \sum_{m=1}^{M}\eta_m[n_m(t)\Psi_{m,1}(t) + Y_{m,1,1}(t)]\right\}\\
& + 2\lambda^{-2}(t)\left\{\eta_0\Psi_{0,2}(t) + \sum_{m=1}^{M}\eta_m[n_m(t)\Psi_{m,2}(t) + Y_{m,2,2}(t)]\right\}.
\end{aligned} \tag{44}$$

Here

$$Y_{m,k,l}(t) = \int_0^t N_m(t,\tau)\Psi_{m,k}^\diamond(t,\tau)\lambda^l(\tau)\,\mathrm{d}\tau. \tag{45}$$

Since expression (43) is independent of spatial coordinates, the equilibrium equations are satisfied identically. The boundary conditions on the lateral surface of the specimen read

$$\sigma_2(t) = \sigma_3(t) = 0. \tag{46}$$

Excluding pressure p eqns (44) and (46), we find the only non-zero component of the Cauchy stress tensor

$$\begin{aligned}
\sigma_1(t) = {} & 2\eta_0[(\lambda^2(t) - \lambda^{-1}(t))\Psi_{0,1}(t) + (\lambda^4(t) - \lambda^{-2}(t))\Psi_{0,2}(t)]\\
& + 2\sum_{m=1}^{M}\eta_m\{[(n_m(t)\Psi_{m,1}(t) + Y_{m,1,-2}(t))\lambda^2(t) - (n_m(t)\Psi_{m,1}(t) + Y_{m,1,1}(t))\lambda^{-1}(t)]\\
& + [(n_m(t)\Psi_{m,2}(t) + Y_{m,2,-4}(t))\lambda^4(t) - (n_m(t)\Psi_{m,2}(t) + Y_{m,2,2}(t))\lambda^{-2}(t)]\}.
\end{aligned} \tag{47}$$

Given program of loading $\lambda = \lambda(t)$, eqn (47) together with eqns (19), (27), (33), (42), and (45) determines the longitudinal stress $\sigma_1(t)$ provided the parameters M, B, β, γ_{m0}, η_m, and the functions $\tilde{W}_m(I_1, I_2)$ are prescribed.

Expression (47) is simplified essentially for the neo-Hookean viscoelastic medium with the strain energy density (34). Assuming additionally that

$$\mu_0 = \mu_1 = \cdots = \mu_M = \mu, \tag{48}$$

we write

$$\sigma_1(t) = \mu\left\{\eta_0[\lambda^2(t) - \lambda^{-1}(t)] + \sum_{m=1}^{M} \eta_m[(n_m(t) + Y_{m,-2}(t))\lambda^2(t) - (n_m(t) + Y_{m,1}(t))\lambda^{-1}(t)]\right\}, \tag{49}$$

where

$$Y_{m,k}(t) = \int_0^t N_m(t,\tau)\lambda^k(\tau)\,d\tau. \tag{50}$$

Combining eqns (19) and (50), we find that the functions $Y_{m,k}(t)$ obey the ordinary differential equations

$$\begin{aligned}\frac{dY_{m,k}}{dt}(t) &= N_m(t,t)\lambda^k(t) + \int_0^t \frac{\partial N_m}{\partial t}(t,\tau)\lambda^k(\tau)\,d\tau \\ &= \gamma_m(t)\lambda^k(t) - \int_0^t \gamma_m(t)N_m(t,\tau)\lambda^k(\tau)\,d\tau \\ &= \gamma_m(t)[\lambda^k(t) - Y_{m,k}(t)], \quad Y_{m,k}(0) = 0.\end{aligned} \tag{51}$$

To calculate the stress $\sigma_1(t)$ for a given function $\lambda(t)$, we should solve ordinary differential equations (19) and (51) with the parameters γ_m calculated according to eqn (27), and substitute the obtained functions $n_m(t)$ and $Y_{m,k}(t)$ into formula (49).

Let us consider the standard relaxation test with

$$\lambda(t) = \begin{cases}\lambda, & t \geqslant 0, \\ 1, & t < 0\end{cases}. \tag{52}$$

It follows from eqns (42), (48), and (52) that

$$\tilde{W}_0 = \frac{\mu}{2}\left(\lambda^2 + \frac{2}{\lambda} - 3\right). \tag{53}$$

Equations (27) and (53) imply that $\gamma_m = \gamma_m(\lambda)$ are independent of time. Integration of eqns (19) and (51) results in

$$n_m(t) = \exp(-\gamma_m t), \quad Y_{m,k}(t) = \lambda^k[1 - \exp(-\gamma_m t)]. \tag{54}$$

Substituting expressions (52) and (54) into eqn (49), we obtain

$$\sigma_1(t) = \mu(\lambda^2 - \lambda^{-1})\left\{\eta_0 + \sum_{m=1}^{M} \eta_m \exp[-\gamma_m(\lambda)t]\right\}. \tag{55}$$

Calculating the logarithm of both sides of eqn (55) and bearing in mind eqn (27), we arrive at the formula

$$\log \sigma_1(t) = \log r(\lambda) + \log\left\{\mu_0\left[\eta_0 + \sum_{m=1}^{M} \eta_m \exp\left(-\frac{\gamma_m(\lambda_0)}{a_0(\lambda)}t\right)\right]\right\}, \tag{56}$$

where λ_0 is a fixed extension ratio, $\mu_0 = \mu(\lambda_0^2 - \lambda_0^{-1})$, log = $\log_{10}$, and

$$r(\lambda) = \frac{\lambda^2 - \lambda^{-1}}{\lambda_0^2 - \lambda_0^{-1}}. \tag{57}$$

It follows from eqn (56) that in the bi-logarithmic coordinates, the relaxation curve corresponding to an arbitrary extension ratio λ can be obtained from the relaxation curve at the extension ratio λ_0 by vertical shift by $\log r(\lambda)$ and horizontal shift by $\log a_0(\lambda)$. The latter means that some master curve can be constructed by vertical and horizontal shifts of an arbitrary set of relaxation curves measured at various extension ratios.

To validate this assertion, we analyze experimental data for poly(methyl methacrylate) plotted in Fig. 1. This figure demonstrates that the material under consideration does not possess the separability property.

The relaxation master curve is depicted in Fig. 2 together with its approximation by the function

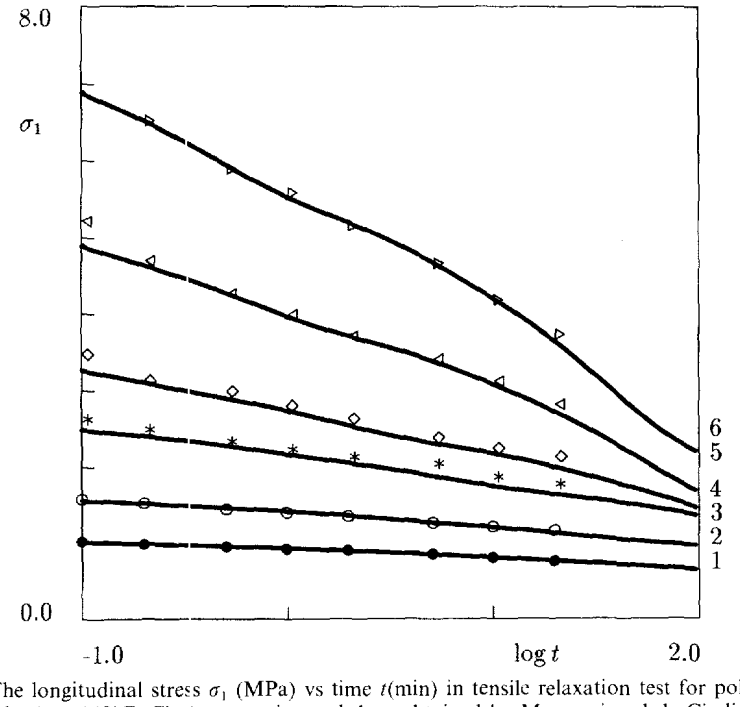

Fig. 1. The longitudinal stress σ_1 (MPa) vs time t(min) in tensile relaxation test for poly(methyl methacrylate) at 140°C. Circles, experimental data obtained by Marrucci and de Cindio (1980); solid lines, prediction of the model. Curve 1, $\lambda = 1.32$; curve 2, $\lambda = 1.59$; curve 3, $\lambda = 2.00$; curve 4, $\lambda = 2.39$; curve 5, $\lambda = 2.91$; curve 6, $\lambda = 3.64$.

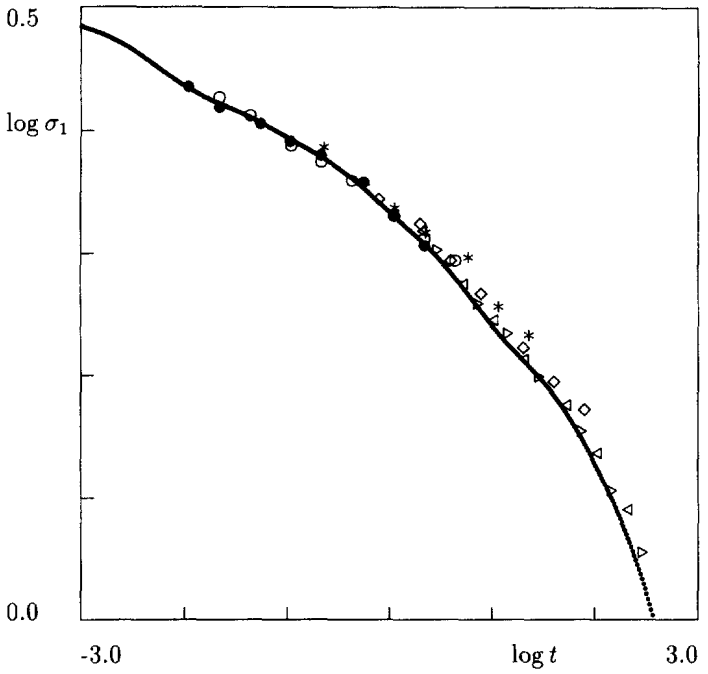

Fig. 2. The longitudinal stress σ_1 (MPa) vs time t (min) in tensile relaxation test for poly(methyl methacrylate) at 140°C. The master curve (reduced to $\lambda = 2.0$) is obtained based on experimental data provided by Marrucci and de Cindio (1980). Filled circles, $\lambda = 1.32$; unfilled circles, $\lambda = 1.59$; asterisks, $\lambda = 2.0$; diamonds, $\lambda = 2.39$; left triangles, $\lambda = 2.91$; right triangles, $\lambda = 3.64$. Solid line: approximation of the master curve by the Prony series with $M = 6$, $\mu_0 = 3.134$ (MPa), and the parameters η_m and $\gamma_m(\lambda_0)$ presented in Table 1.

Table 1. The adjustable parameters η_m and $\gamma_m(\lambda_0)$ for poly(methyl methacrylate) at 140°C

η_m	$\gamma_m(\lambda_0)$ (min^{-1})
0.1962	0.000
0.2753	0.002
0.0900	0.020
0.1450	0.200
0.1000	2.000
0.0641	20.000
0.1295	200.000

$$\mu_0 \left[\eta_0 + \sum_{m=1}^{M} \eta_m \exp(-\gamma_m(\lambda_0) t) \right]$$

with $M = 6$. The adjustable parameters μ_0, η_m, and $\gamma_m(\lambda_0)$ are found to ensure the best fit of experimental data.

To check that the neo-Hookean model eqns (34) and (48) can be applied to describe the behavior of poly(methyl methacrylate), we plot the ratio r obtained by vertical shift of the relaxation curves vs the ratio

$$\frac{\lambda^2 - \lambda^{-1}}{\lambda_0^2 - \lambda_0^{-1}}.$$

The results presented in Fig. 3 make evident that formula (57) is satisfied with a high level of accuracy.

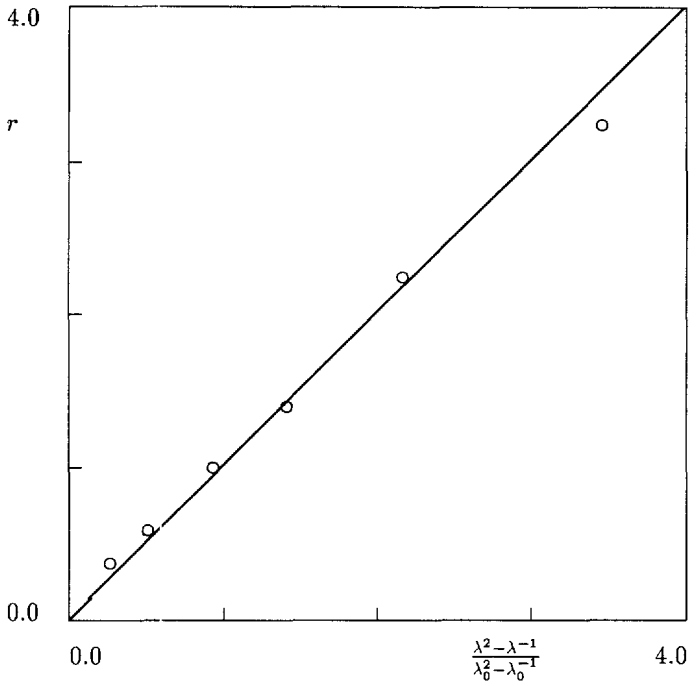

Fig. 3. The ratio of the elastic response at the extension ratio λ to the elastic response at the elastic ratio λ_0 vs the ratio $(\lambda^2-\lambda^{-1})(\lambda_0^2-\lambda_0^{-1})^{-1}$ for poly(methyl methacrylate) at 140°C. Circles, data obtained by vertical shift of the relaxation curves; solid line, prediction of the model.

The shift factor a_0 determined by horizontal shift of the relaxation curves is plotted in Fig. 4 vs the strain energy density $\tilde{W}_0$. Figure 4 shows that the phenomenological eqn (23) with adjustable parameters B and β correctly predicts the effect of strains on the relaxation spectrum.

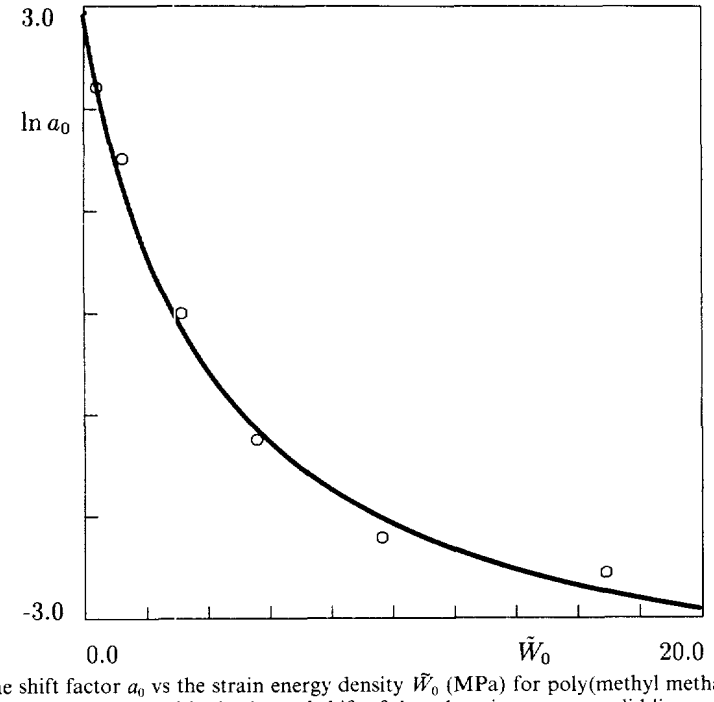

Fig. 4. The shift factor a_0 vs the strain energy density $\tilde{W}_0$ (MPa) for poly(methyl methacrylate) at 140°C. Circles, data obtained by horizontal shift of the relaxation curves; solid line, prediction of the model with $B_0 = 2.978$, $B = 7.092$, and $\beta = 0.245$.

The relaxation curves calculated according to eqn (55) are plotted in Fig. 1. This figure demonstrates fair agreement between experimental data and their prediction by the model.

Another issue of interest is an opportunity to describe yield of viscoelastic–plastic media using some "internal clock". As common practice, the material yield is treated as a local maximum on the nominal stress–nominal strain diagram in tension with a constant rate of strains. The first model with a stress-dependent relaxation spectrum for the yield-like behavior of viscoelastic media was proposed by Tobolsky and Eyring (1943). This concept has been developed by Bernstein and Shokooh (1980) and, recently, by Hasan *et al.* (1993) and Tervoort *et al.* (1996), to mention a few. To describe yield in polymeric media, nonlinear integral constitutive models with strain-dependent spectra were suggested by Shay and Caruthers (1986) and Wineman and Waldron (1993, 1995). Since the fact that integral constitutive relations in nonlinear viscoelasticity can model the material yield provided the relaxation times depend on stresses (strains) has already become evident, we concentrate on the so-called double yield, where two points of maximum can be found on the nominal stress–nominal strain diagram prior to necking. The double yield under tensile loading was observed in polyethylene and its copolymers, see Brooks *et al.* (1992, 1995), Lucas *et al.* (1995), Seguela and Rietsch (1990), Truss *et al.* (1984), and Wilding and Ward (1981), and in poly(tetramethylene terephthalate) and its copolymers, see Muramatsu and Lando (1995). Secondary crystallization of polymers appears to be a driving force for this phenomenon (e.g., Lucas *et al.*, 1995).

To demonstrate opportunities of the constitutive model (49), we fit experimental data for ethylene–octene and ethylene–butene copolymers in tension with a constant rate of nominal strains $\dot{\varepsilon}$,

$$\lambda(t) = 1 + \dot{\varepsilon} t. \tag{58}$$

Since the number of experimental data for any test is not large (from 10 to 20), we confine ourselves to the cases $M = 1$ (one kind of replacing links). In this case, eqn (49) reads

$$\sigma_1(t) = C_1 q_1(t) + C_2 q_2(t). \tag{59}$$

Here

$$q_1(t) = \lambda^2(t) - \lambda^{-1}(t),$$

$$q_2(t) = [n_1(t) + y_2(t)]\lambda^2(t) - [n_1(t) + y_1(t)]\lambda^{-1}(t),$$

where the functions $n_1(t)$, $y_1(t) = Y_{1,1}(t)$, and $y_2(t) = Y_{1,-2}(t)$ obey the ordinary differential equations

$$\frac{dn_1}{dt} = -\gamma_1(t) n_1, \quad n_1(0) = 1,$$

$$\frac{dy_1}{dt} = \gamma_1(t)[\lambda(t) - y_1], \quad y_1(0) = 0,$$

$$\frac{dy_2}{dt} = \gamma_1(t)[\lambda^{-2}(t) - y_2], \quad y_2(0) = 0.$$

The function $\gamma_1(t)$ is calculated as

$$\gamma_1(t) = \frac{\gamma_{10}}{a(t)},$$

where

$$\ln a(t) = B\left[\frac{1}{1+\beta_0(\lambda^2(t)+2\lambda^{-1}(t)-3)}-1\right].$$

The constants C_1, C_2, and β_0 are expressed in terms of the model parameters as

$$C_1 = \mu(1-\eta_1), \quad C_2 = \mu\eta_1, \quad \beta_0 = \tfrac{1}{2}\mu\beta.$$

Given γ_{10}, B, and β_0, the adjustable parameters C_1 and C_2 are found by using the least squares method. To determine the parameters γ_{10}, B, and β_0, which ensure the best approximation of experimental data, we employ a version of the steepest descent method with constrains $C_1 \geqslant 0$ and $C_2 \geqslant 0$.

Experimental data and their prediction by the model are plotted in Figs 5 and 6. It should be noted here that two local maxima are observed only on the nominal stress–nominal strain curves, see, e.g. Figs 1 and 2 in Lucas *et al.* (1995), while the true stress–extension ratio dependencies reveal rather a "quasi-yield" behavior, see Figs 5 and 6.

The following conclusions may be drawn:

(i) the model (49) with a strain-dependent relaxation spectrum correctly describes double yield in polymers even when only one kind of adaptive links is taken into account;
(ii) the effect of strains on the relaxation spectrum increases abruptly when the specimen under consideration demonstrates double yield.

Since double yield is typical of semicrystalline polymers, a hypothesis may be suggested that a significant deviation of the viscoelastic behavior of polymers from the separability property is caused by (or, at least, is connected with) high level of crystallinity.

To make evident that the model does not only fit experimental data, but adequately predicts the material response, we determine adjustable parameters by using results of tensile test with one rate of strains, calculate the longitudinal stress in tensile test with another rate of strains, and compare results of numerical simulation with experimental

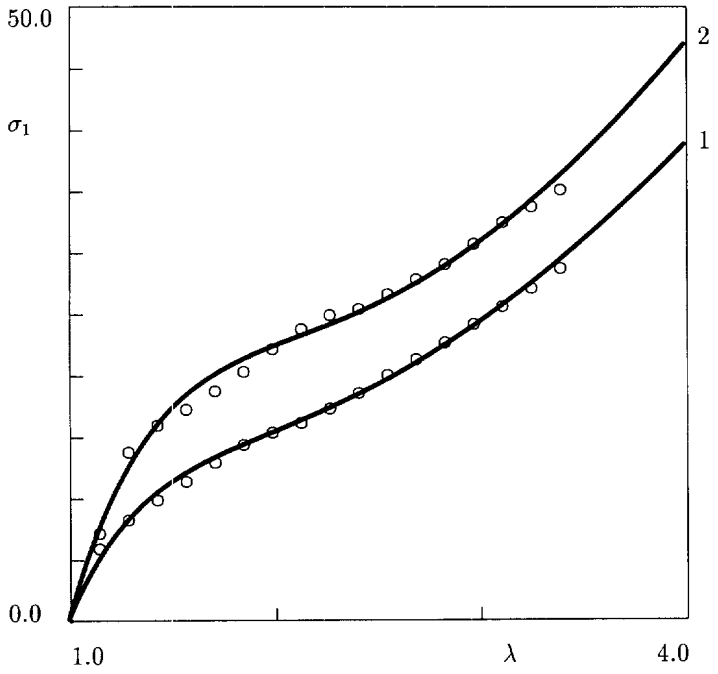

Fig. 5. The longitudinal stress σ_1 (MPa) vs the extension ratio λ for ethylene–octene copolymer in tension with the rate of strain $\dot{\varepsilon} = 0.085$ (s^{-1}) at 25°C. Circles, experimental data obtained by Lucas *et al.* (1995), solid lines, prediction of the model. Curve 1—core crystallinity 0.27, $\mu = 13.630$ (MPa), $\gamma_{10} = 0.28$ (s^{-1}), $\eta_1 = 0.834$, $B = 0.0$, and $\beta_0 = 0.0$; curve 2—core crystallinity 0.40, $\mu = 20.028$ (MPa), $\gamma_{10} = 0.24$ (s^{-1}), $\eta_1 = 0.866$, $B = 0.22$, and $\beta_0 = 0.24$.

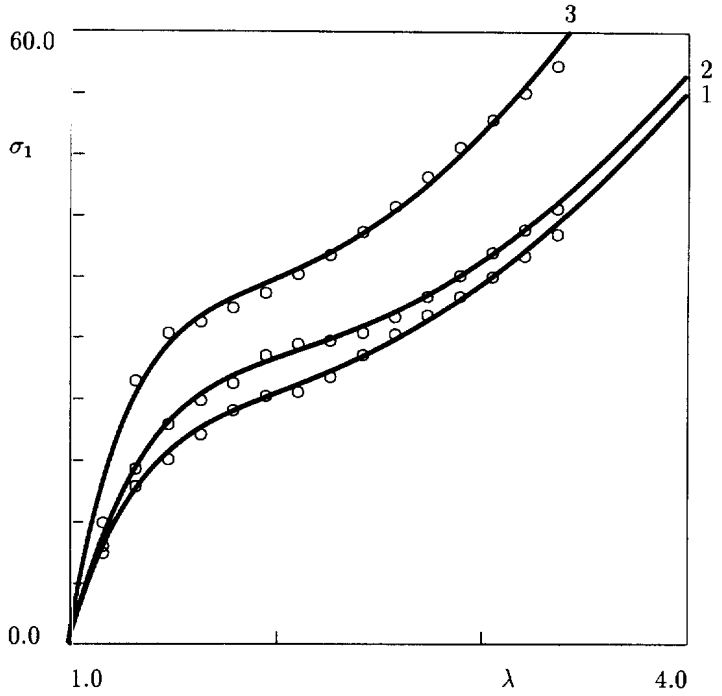

Fig. 6. The longitudinal stress σ_1 (MPa) vs the extension ratio λ for ethylene–butene copolymer in tension with the rate of strain $\dot{\varepsilon} = 0.085$ (s^{-1}) at 25°C. Circles, experimental data obtained by Lucas *et al.* (1995), solid lines, prediction of the model. Curve 1—core crystallinity 0.36, $\mu = 23.921$ (MPa), $\gamma_{10} = 0.28$ (s^{-1}), $\eta_1 = 0.87$, $B = 0.0$ and $\beta_0 = 0.0$; curve 2—core crystallinity 0.44, $\mu = 24.379$ (MPa), $\gamma_{10} = 0.18$ (s^{-1}), $\eta_1 = 0.87$, $B = 0.34$, and $\beta_0 = 5.8$; curve 3—core crystallinity 0.55, $\mu = 41.264$ (MPa), $\gamma_{10} = 0.32$ (s^{-1}), $\eta_1 = 0.90$, $B = 0.0$, and $\beta_0 = 0.0$.

data. The curves plotted in Fig. 7 for poly(ethylene terephthalate) show that the model ensures good agreement between experimental data and numerical prediction for strains up to 100 per cent when the rates of strains differ by more than an order.

To demonstrate ability of the model to predict the viscoelastic behavior under different loading programs, we determine adjustable parameters by using data in the standard relaxation test, calculate the material response in tensile test with a constant rate of strains, and compare results of numerical simulation with observations. Since appropriate data at finite strains are not available, we confine ourselves to small deformations (up to 4 per cent) of a polycarbonate specimen. The mechanical behavior of adaptive links under uniaxial loading is modeled by the nonlinear constitutive relation

$$\sigma = K|\varepsilon|^{\alpha} \operatorname{sign} \varepsilon, \tag{60}$$

where σ is the nominal stress, ε is the nominal strain, and K and α are material parameters, see Drozdov (1997). Experimental data together with their prediction by the model with $M = 6$ are plotted in Fig. 8 for the standard relaxation test and in Fig. 9 for the tensile test with constant rate of strains. Figure 9 shows good agreement between observations and results of numerical simulation. The maximal difference between measured and calculated stresses does not exceed 10 per cent, which is quite acceptable taking into account that only four relaxation curves were available to construct the master curve.

6. SIMPLE SHEAR OF A SPECIMEN

As another example of homogeneous deformations, we consider simple shear of a viscoelastic medium

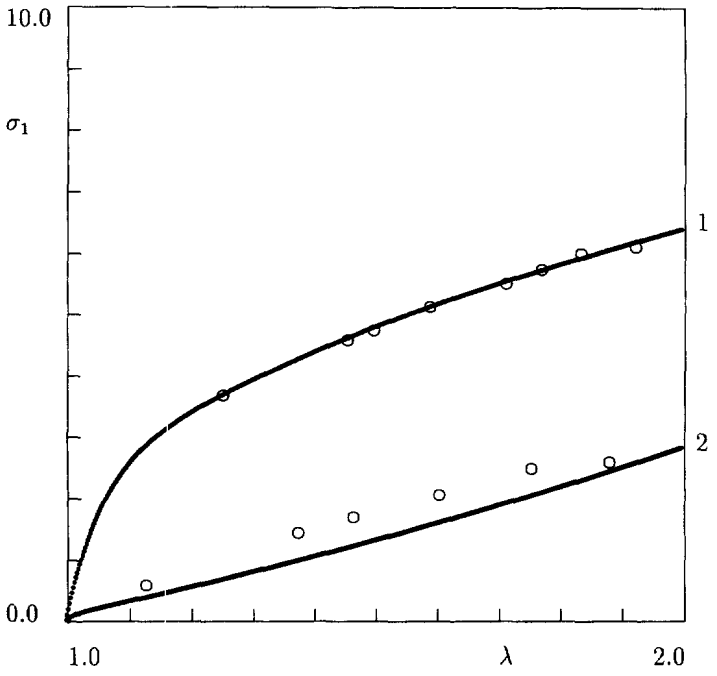

Fig. 7. The longitudinal stress σ_1 (MPa) vs the extension ratio λ for poly(ethylene terephthalate) in tension at 90°C with a constant rate of strain $\dot{\varepsilon}$. Circles, experimental data obtained by Salem (1992); solid lines, prediction of the model with $M = 2$. Curve 1, $\dot{\varepsilon} = 0.42$ (s^{-1}); curve 2, $\dot{\varepsilon} = 0.01$ (s^{-1}). The adjustable parameters $\mu = 16.395$ (MPa), $\eta_1 = 0.803$, $\eta_2 = 0.149$, $B = 0.1$, and $\beta_0 = 12.0$ are found by fitting experimental data for $\dot{\varepsilon} = 0.42$ (s^{-1}) with $\gamma_{10} = 8.0$ (s^{-1}) and $\gamma_{20} = 0.8$ (s^{-1}).

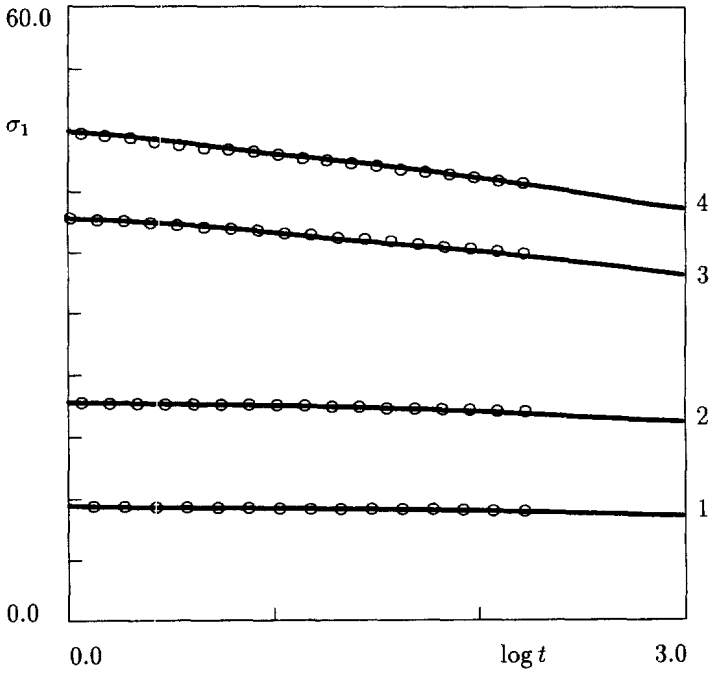

Fig. 8. The longitudinal stress σ_1 (MPa) vs time t (min) in tensile relaxation test for polycarbonate at 20°C. Circles, experimental data obtained by Tervoort *et al.* (1996); solid lines, prediction of the model. Curve 1, $\varepsilon = 0.005$; curve 2, $\varepsilon = 0.010$, curve 3, $\varepsilon = 0.021$; curve 4, $\varepsilon = 0.029$. The adjustable parameters of the model equal $K = 1404.302$ (MPa), $\alpha = 0.837$, $B_0 = 1.092$, $B = 8.904$, and $\beta = 1.18$. The relaxation master curve (reduced to $\varepsilon = 0.01$) is approximated by the Prony series with $M = 6$ and the parameters η_m and γ_{m0} presented in Table 2.

Table 2. The adjustable parameters η_m and γ_{m0} for polycarbonate at 20°C

η_m	γ_{m0} (min^{-1})
0.5807	0.00000
0.0602	0.00005
0.0272	0.00050
0.0347	0.00500
0.0086	0.05000
0.0087	0.50000
0.2798	5.00000

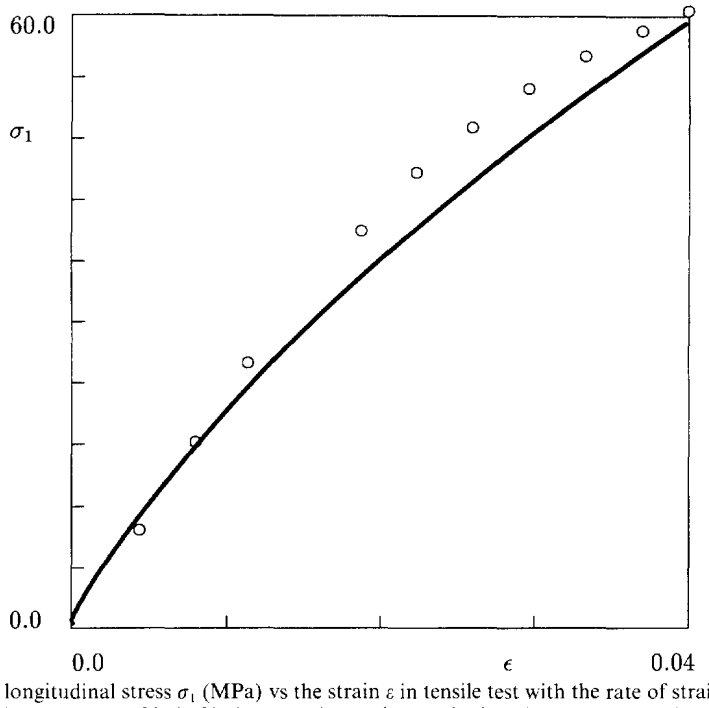

Fig. 9. The longitudinal stress σ_1 (MPa) vs the strain ε in tensile test with the rate of strain $\dot{\varepsilon} = 0.01$ (s^{-1}) for polycarbonate at 20°C. Circles, experimental data obtained by Tervoort *et al.* (1996); solid line, prediction of the model.

$$x^1 = X^1 + \kappa(t)X^2, \quad x^2 = X^2, \quad x^3 = X^3, \tag{61}$$

where X^i and x^i are Cartesian coordinates in the initial and actual configurations, and $\kappa = \kappa(t)$ is a coefficient of shear.

It follows from eqn (61) that the deformation gradient $\bar{\nabla}_0\bar{r}(t)$ from the initial to the actual configuration at instant t and the deformation gradient $\bar{\nabla}_\tau\bar{r}(t)$ from the actual configuration at instant τ to the actual configuration at instant t are determined by the formulas

$$\bar{\nabla}_0\bar{r}(t) = \mathbf{I} + \kappa(t)\bar{\mathbf{e}}_2\bar{\mathbf{e}}_1, \quad \bar{\nabla}_\tau\bar{r}(t) = \mathbf{I} + [\kappa(t) - \kappa(\tau)]\bar{\mathbf{e}}_2\bar{\mathbf{e}}_1, \tag{62}$$

where $\mathbf{I}$ is the unit tensor, and $\bar{\mathbf{e}}_i$ are unit vectors of the Cartesian coordinate frame in the initial configuration.

According to eqn (62), the Finger tensors $\mathbf{F}^0(t)$ and $\mathbf{F}^\circ(t, \tau)$ equal

$$\mathbf{F}^0(t) = \mathbf{I} + \kappa^2(t)\bar{\mathbf{e}}_1\bar{\mathbf{e}}_1 + \kappa(t)(\bar{\mathbf{e}}_1\bar{\mathbf{e}}_2 + \bar{\mathbf{e}}_2\bar{\mathbf{e}}_1),$$

$$\mathbf{F}^\circ(t,\tau) = \mathbf{I} + [\kappa(t) - \kappa(\tau)]^2\bar{\mathbf{e}}_1\bar{\mathbf{e}}_1 + [\kappa(t) - \kappa(\tau)](\bar{\mathbf{e}}_1\bar{\mathbf{e}}_2 + \bar{\mathbf{e}}_2\bar{\mathbf{e}}_1). \tag{63}$$

Equation (63) implies that

$$I_1^0(t) = I_2^0(t) = 3 + \kappa^2(t), \quad I_3^0(t) = 1,$$

$$I_1^\circ(t,\tau) = I_2^\circ(t,\tau) = 3 + [\kappa(t) - \kappa(\tau)]^2, \quad I_3^\circ(t,\tau) = 1. \tag{64}$$

We confine ourselves to a neo-Hookean viscoelastic medium eqns (34) and (48) with a strain-dependent relaxation spectrum. Combining eqns (35), (48), (63), and (64), we find that

$$\boldsymbol{\sigma}(t) = \sigma_{11}(t)\bar{\mathbf{e}}_1\bar{\mathbf{e}}_1 + \sigma_{22}(t)\bar{\mathbf{e}}_2\bar{\mathbf{e}}_2 + \sigma_{33}(t)\bar{\mathbf{e}}_3\bar{\mathbf{e}}_3 + \sigma_{12}(t)(\bar{\mathbf{e}}_1\bar{\mathbf{e}}_2 + \bar{\mathbf{e}}_2\bar{\mathbf{e}}_1), \tag{65}$$

where

$$\sigma_{11}(t) = -p(t) + \mu\left\{\left[\eta_0 + \sum_{m=1}^{M}\eta_m n_m(t)\right][1 + \kappa^2(t)] + \sum_{m=1}^{M}\eta_m\int_0^t N_m(t,\tau)[1 + (\kappa(t) - \kappa(\tau))^2]\,\mathrm{d}\tau\right\},$$

$$\sigma_{22}(t) = \sigma_{33}(t) = -p(t) + \mu\left\{\eta_0 + \sum_{m=1}^{M}\eta_m\left[n_m(t) + \int_0^t N_m(t,\tau)\,\mathrm{d}\tau\right]\right\},$$

$$\sigma_{12}(t) = \mu\left\{\left[\eta_0 + \sum_{m=1}^{M}\eta_m n_m(t)\right]\kappa(t) + \sum_{m=1}^{M}\eta_m\int_0^t N_m(t,\tau)[\kappa(t) - \kappa(\tau)]\,\mathrm{d}\tau\right\}. \tag{66}$$

It follows from eqn (66) that the first difference of normal stresses equals

$$\Delta\sigma(t) = \mu\left\{\left[\eta_0 + \sum_{m=1}^{M}\eta_m n_m(t)\right]\kappa^2(t) + \sum_{m=1}^{M}\eta_m\int_0^t N_m(t,\tau)[\kappa(t) - \kappa(\tau)]^2\,\mathrm{d}\tau\right\}. \tag{67}$$

Substitution of expressions (64) into eqn (34) with the use of eqn (48) yields

$$\tilde{W}_0 = \tfrac{1}{2}\mu\kappa^2. \tag{68}$$

Given shear history $\kappa(t)$, eqns (65) and (66) together with eqns (19), (27), and (68) determine stresses in a viscoelastic medium. Since components of the Cauchy stress tensor $\boldsymbol{\sigma}$ are independent of spatial coordinates, the equilibrium equations are satisfied identically.

Let us consider the standard relaxation test with

$$\kappa(t) = \begin{cases}\kappa, & t \geqslant 0,\\ 0, & t < 0.\end{cases} \tag{69}$$

Substituting expression (69) into eqn (66), we find that

$$\sigma_{12}(t) = \mu\kappa\left[\eta_0 + \sum_{m=1}^{M}\eta_m n_m(t)\right]. \tag{70}$$

According to eqns (68) and (70), the strain energy density $\tilde{W}_0$ is independent of time, which

implies that the rates of reformation $\gamma_m = \gamma_m(\kappa)$ are time-dependent as well. Integration of eqn (19) yields

$$n_m(t) = \exp[-\gamma_m(\kappa)t]. \tag{71}$$

We substitute expression (71) into eqn (70) and arrive at the formula

$$\sigma_{12}(t) = \mu\kappa\left\{\eta_0 + \sum_{m=1}^{M} \eta_m \exp[-\gamma_m(\kappa)t]\right\}. \tag{72}$$

Calculating the logarithm of both sides of eqn (72), we obtain

$$\log\sigma_{12}(t) = \log r(\kappa) + \log\left\{\mu_0\left[\eta_0 + \sum_{m=1}^{M} \eta_m \exp\left(-\frac{\gamma_m(\kappa_0)}{a_0(\kappa)}t\right)\right]\right\}, \tag{73}$$

where κ_0 is a fixed coefficient of shear, $\mu_0 = \mu\kappa_0$, and

$$r(\kappa) = \frac{\kappa}{\kappa_0}. \tag{74}$$

Equation (73) implies that in the bi-logarithmic coordinates, the relaxation curve at an arbitrary coefficient of shear κ is obtained from the relaxation curve at κ_0 by vertical shift by $\log r(\kappa)$ and by horizontal shift by $\log a_0(\kappa)$. The latter means that some master curve can be constructed by vertical and horizontal shifts of relaxation curves measured at various coefficients of shear.

To examine this assertion, we consider experimental data for poly(methyl methacrylate) plotted in Fig. 10. The relaxation master curve is depicted in Fig. 11 together with its approximation by the function

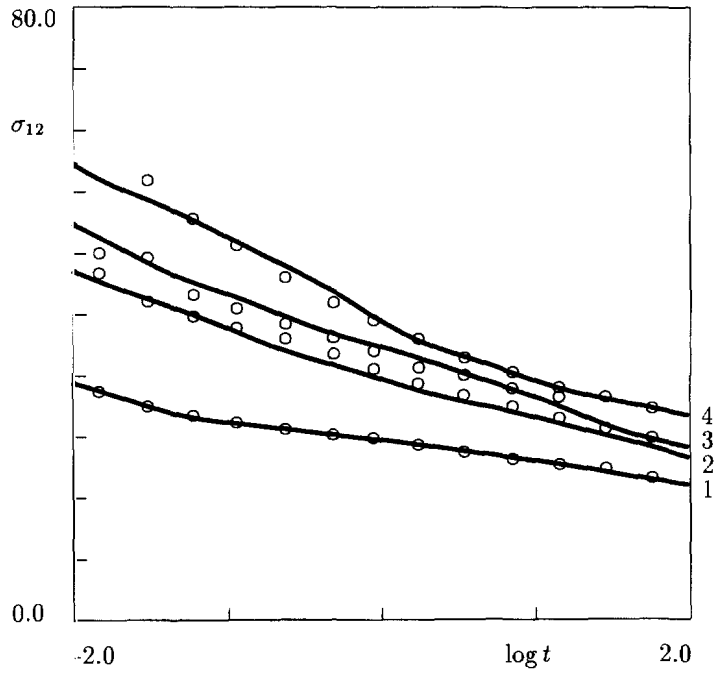

Fig. 10. The shear stress σ_{12} (MPa) vs time t (min) for poly(methyl methacrylate) at 24°C. Circles, experimental data obtained by McKenna and Zapas (1979); solid lines, prediction of the model. Curve 1, $\kappa = 0.03$; curve 2, $\kappa = 0.05$, $\kappa = 0.06$; curve 4, $\kappa = 0.10$.

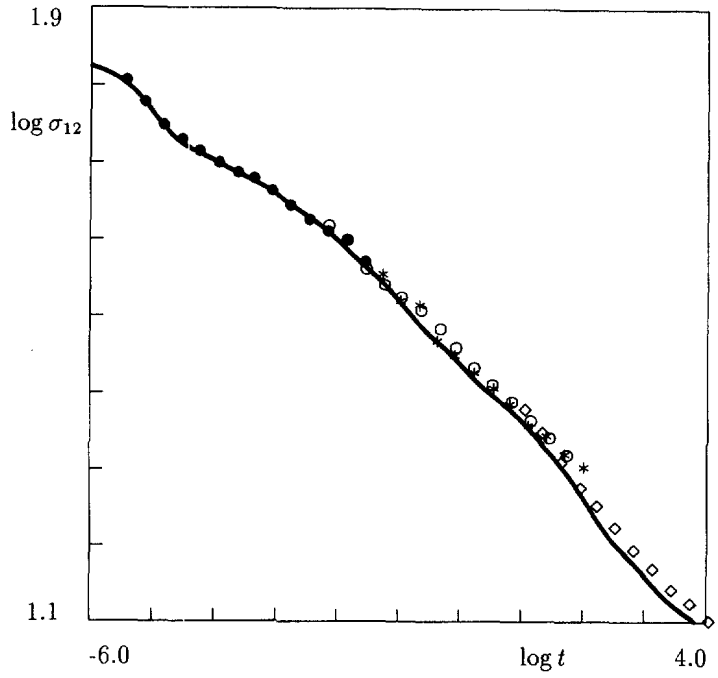

Fig. 11. The shear stress σ_{12} (MPa) vs time t (min) for poly(methyl methacrylate) at 24°C. The master curve (reduced to $\kappa_0 = 0.05$) is obtained based on experimental data provided by McKenna and Zapas (1979). Filled circles, $\kappa = 0.03$; unfilled circles, $\kappa = 0.05$; asterisks, $\kappa = 0.06$; diamonds, $\kappa = 0.10$. Solid line: approximation of the master curve by the Prony series with $M = 10$, $\mu_0 = 68.334$ (MPa), and the parameters η_m and $\gamma_m(\kappa_0)$ presented in Table 3.

Table 3. The adjustable parameters η_m and $\gamma_m(\kappa_0)$ for poly(methyl methacrylate) at 24°C

η_m	$\gamma_m(\kappa_0)$ (min^{-1})
0.1687	0.0000
0.0318	0.0001
0.0456	0.0010
0.0842	0.0100
0.0527	0.1000
0.0776	1.0000
0.1036	10.0000
0.0891	100.0000
0.0721	1000.0000
0.0627	10,000.0000
0.2118	100,000.0000

$$\mu_0 \left[\eta_0 + \sum_{m=1}^{M} \eta_m \exp(-\gamma_m(\lambda_0)t) \right]$$

with $M = 10$. The adjustable parameters μ_0, η_m, and $\gamma_m(\kappa_0)$ are found to ensure the best fit of experimental data. To check that the neo-Hookean model eqns (34) and (48) correctly describe the mechanical behavior of poly(methyl methacrylate), the ratio r obtained by vertical shift of the relaxation curves is plotted vs the ratio κ/κ_0 in Fig. 12. The results presented in this figure demonstrate that formula (74) is satisfied with a high level of accuracy. Finally, to validate the phenomenological equation (23), we depicted the shift factor a_0 determined by horizontal shift of the relaxation curves vs the strain energy density $\tilde{W}_0$, see Fig. 13. The relaxation curves calculated by eqn (72) are plotted in Fig. 10.

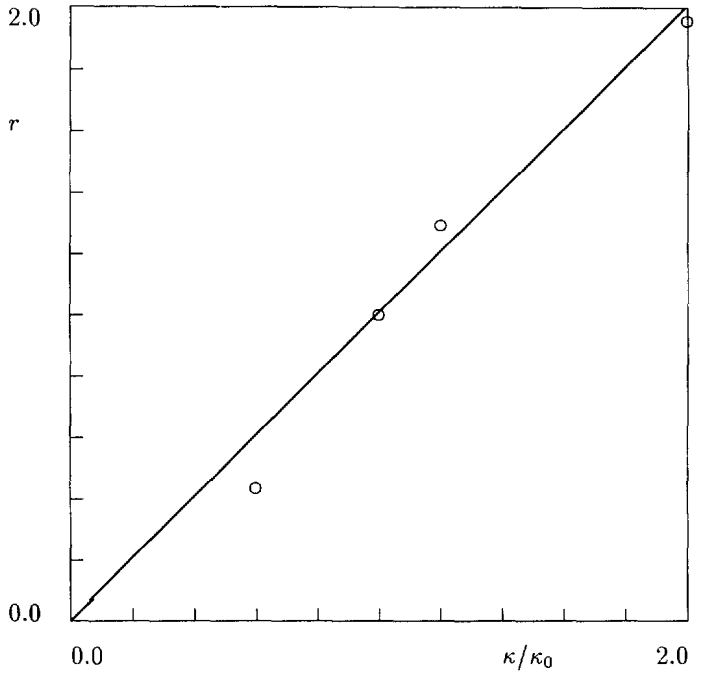

Fig. 12. The ratic r of the elastic response at shear κ to the elastic response at shear $\kappa_0 = 0.05$ vs κ/κ_0 for poly(methyl methacrylate) at 24°C. Circles, data obtained by vertical shift of the relaxation curves; solid line, prediction of the linear model.

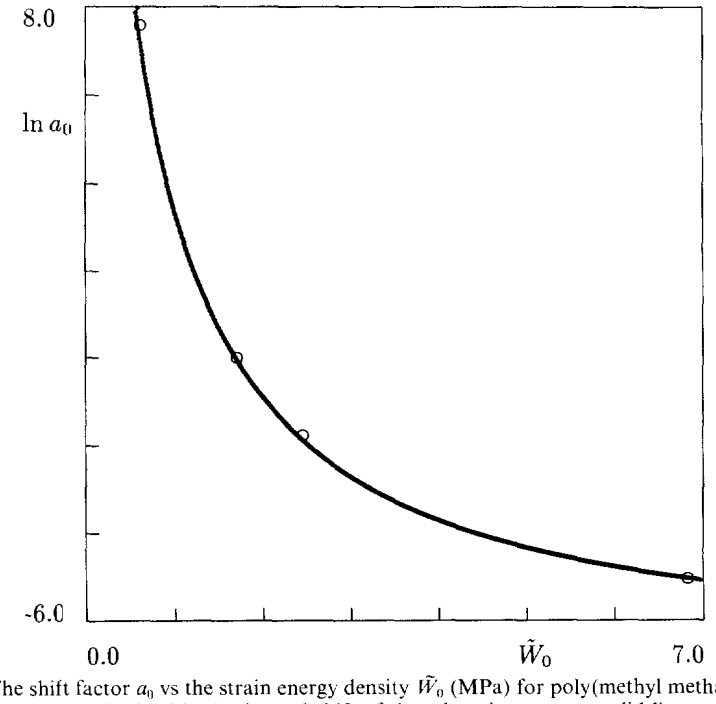

Fig. 13. The shift factor a_0 vs the strain energy density $\tilde{W}_0$ (MPa) for poly(methyl methacrylate) at 24°C. Circles, data obtained by horizontal shift of the relaxation curves; solid line, prediction of the model with $B_0 = 28.891$, $B = 36.032$, and $\beta = 2.350$.

To show that the model describes adequately the nonlinear viscoelastic behavior of other polymers as well, we present data for an epoxy glass. Omitting technical details, we plot only results of the shear relaxation test and their fitting by the model, see Fig. 14. Figures

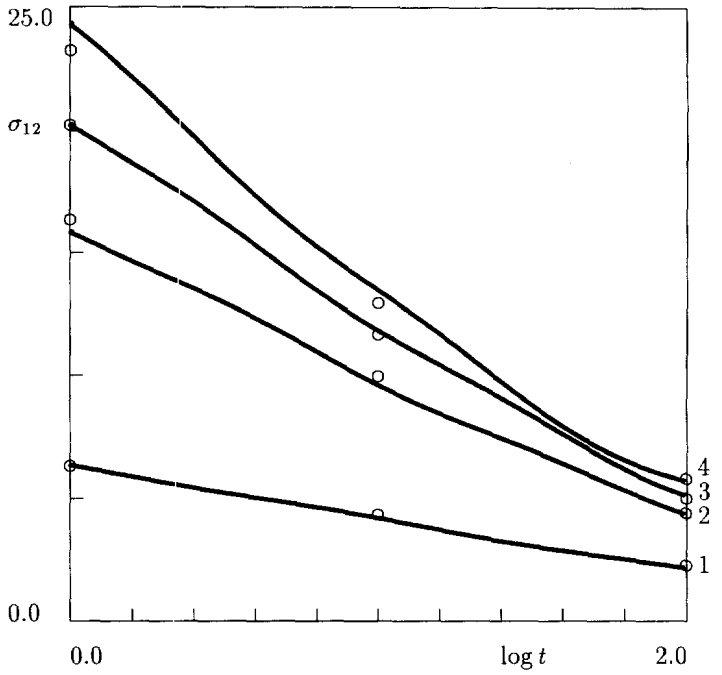

Fig. 14. The shear stress σ_{12} (MPa) vs time t (s) for an epoxy glass at 33.5°C. Circles, experimental data obtained by Waldron *et al.* (1995); solid lines, prediction of the model. Curve 1, $\kappa = 0.01$; curve 2, $\kappa = 0.03$; curve 3, $\kappa = 0.04$; curve 4, $\kappa = 0.05$. The adjustable parameters of the model equal $\mu = 741.137$ (MPa), $B_0 = 0.940$, $B = 4.129$, and $\beta = 0.822$. The relaxation master curve (reduced to $\kappa_0 = 0.03$) is approximated by the Prony series with $M = 4$ and the parameters η_m and γ_{m0} presented in Table 4.

Table 4. The adjustable parameters η_m and γ_{m0} for an epoxy glass at 33.5 °C

η_m	γ_{m0} (s^{-1})
0.0843	0.000
0.0947	0.002
0.2658	0.020
0.2931	0.200
0.2621	2.000

10 and 14 demonstrate fair agreement between experimental data and their prediction by the model.

7. RADIAL DEFORMATION OF A SPHERICAL PRESSURE VESSEL

Sections 5 and 6 dealt with homogeneous deformations of viscoelastic media, where the internal time was the same for all material portions. The latter meant that the aging/rejuvenation processes were homogeneous, and no additional forces arose due to the difference in the material properties at different points. On the other hand, it is well known that inhomogeneous aging can affect significantly stress distribution in a viscoelastic solid (e.g., Arutyunyan *et al.*, 1987).

To analyze stresses built-up due to the inhomogeneity of strains in a viscoelastic medium with an internal clock, we consider inflation of a thick-walled spherical pressure vessel which occupies the domain

$$\{R_1 \leqslant R \leqslant R_2, \quad 0 \leqslant \Theta < 2\pi, \quad 0 \leqslant \Phi \leqslant \pi\}$$

in the initial configuration. Here $\{R, \Theta, \Phi\}$ are spherical coordinates with unit vectors $\bar{\mathbf{e}}_R$, $\bar{\mathbf{e}}_\Theta$, and $\bar{\mathbf{e}}_\Phi$. At the instant $t = 0$, a pressure $p = p(t)$ is applied to the internal surface of the sphere. Spherical coordinates $\{r, \theta, \phi\}$ in the actual configuration are expressed in terms of the Lagrangian coordinates as

$$r = f(t, R), \quad \theta = \Theta, \quad \phi = \Phi, \tag{75}$$

where $f(t, R)$ is a function to be found.

It follows from eqn (75) that the deformation gradient $\bar{\nabla}_0 \bar{r}(t)$ for transition from the initial to the actual configuration at instant t and the deformation gradient $\bar{\nabla}_\tau \bar{r}(t)$ for transition from the actual configuration at instant τ to the actual configuration at instant t equal

$$\bar{\nabla}_0 \bar{r}(t) = h(t)\bar{\mathbf{e}}_R\bar{\mathbf{e}}_R + \frac{f(t)}{R}(\bar{\mathbf{e}}_\Theta\bar{\mathbf{e}}_\Theta + \bar{\mathbf{e}}_\Phi\bar{\mathbf{e}}_\Phi),$$

$$\bar{\nabla}_\tau \bar{r}(t) = \frac{h(t)}{h(\tau)}\bar{\mathbf{e}}_R\bar{\mathbf{e}}_R + \frac{f(t)}{f(\tau)}(\bar{\mathbf{e}}_\Theta\bar{\mathbf{e}}_\Theta + \bar{\mathbf{e}}_\Phi\bar{\mathbf{e}}_\Phi). \tag{76}$$

Here

$$h(t) = \frac{\partial f}{\partial R}(t),$$

and the argument R is omitted for simplicity. Equation (76) implies that

$$\mathbf{F}^0(t) = h^2(t)\bar{\mathbf{e}}_R\bar{\mathbf{e}}_R + \left(\frac{f(t)}{R}\right)^2(\bar{\mathbf{e}}_\Theta\bar{\mathbf{e}}_\Theta + \bar{\mathbf{e}}_\Phi\bar{\mathbf{e}}_\Phi),$$

$$\mathbf{F}^\circ(t, \tau) = \left(\frac{h(t)}{h(\tau)}\right)^2\bar{\mathbf{e}}_R\bar{\mathbf{e}}_R + \left(\frac{f(t)}{f(\tau)}\right)^2(\bar{\mathbf{e}}_\Theta\bar{\mathbf{e}}_\Theta + \bar{\mathbf{e}}_\Phi\bar{\mathbf{e}}_\Phi). \tag{77}$$

According to eqn (77), we can write

$$I_3^0(t) = h^2(t)\left(\frac{f(t)}{R}\right)^4.$$

This equality together with the incompressibility condition (40) results in

$$\frac{\partial f}{\partial R}(t, R) = \left(\frac{R}{f(t, R)}\right)^2. \tag{78}$$

Integration of eqn (78) implies that

$$f^3(t, R) = R^3 + C(t), \tag{79}$$

where $C = C(t)$ is a function to be found. It follows from eqn (79) that

$$f(t,R)=(R^3+C(t))^{1/3},\quad h(t,R)=\left(\frac{R}{f(t,R)}\right)^2. \tag{80}$$

Combining eqns (77) and (80), we arrive at the formulas

$$\mathbf{F}^0(t)=\left(\frac{R}{f(t)}\right)^4\bar{\mathbf{e}}_R\bar{\mathbf{e}}_R+\left(\frac{f(t)}{R}\right)^2(\bar{\mathbf{e}}_\Theta\bar{\mathbf{e}}_\Theta+\bar{\mathbf{e}}_\Phi\bar{\mathbf{e}}_\Phi),$$

$$\mathbf{F}^\diamond(t,\tau)=\left(\frac{f(\tau)}{f(t)}\right)^4\bar{\mathbf{e}}_R\bar{\mathbf{e}}_R+\left(\frac{f(t)}{f(\tau)}\right)^2(\bar{\mathbf{e}}_\Theta\bar{\mathbf{e}}_\Theta+\bar{\mathbf{e}}_\Phi\bar{\mathbf{e}}_\Phi).$$

$$I_1^0(t)=\left(\frac{R}{f(t)}\right)^4+2\left(\frac{f(t)}{R}\right)^2,\quad I_2^0(t)=\left(\frac{f(t)}{R}\right)^4+2\left(\frac{R}{f(t)}\right)^2,$$

$$I_1^\diamond(t,\tau)=\left(\frac{f(\tau)}{f(t)}\right)^4+2\left(\frac{f(t)}{f(\tau)}\right)^2,\quad I_2^\diamond(t,\tau)=\left(\frac{f(t)}{f(\tau)}\right)^4+2\left(\frac{f(\tau)}{f(t)}\right)^2. \tag{81}$$

Substitution of expressions (81) into the constitutive eqn (35) yields

$$\boldsymbol{\sigma}(t)=\sigma_R(t)\bar{\mathbf{e}}_R\bar{\mathbf{e}}_R+\sigma_\Theta(t)\bar{\mathbf{e}}_\Theta\bar{\mathbf{e}}_\Theta+\sigma_\Phi(t)\bar{\mathbf{e}}_\Phi\bar{\mathbf{e}}_\Phi, \tag{82}$$

where

$$\sigma_R(t)=-p(t)+\mu\left(\frac{R}{f(t)}\right)^4\left\{\eta_0+\sum_{m=1}^{M}\eta_m[n_m(t)+Y_{m,4}(t)]\right\},$$

$$\sigma_\Theta(t)=\sigma_\Phi(t)=-p(t)+\mu\left(\frac{f(t)}{R}\right)^2\left\{\eta_0+\sum_{m=1}^{M}\eta_m[n_m(t)+Y_{m,-2}(t)]\right\}, \tag{83}$$

where

$$Y_{m,k}(t)=\int_0^t N_m(t,\tau)\left(\frac{f(\tau)}{R}\right)^k\mathrm{d}\tau. \tag{84}$$

It follows from eqn (83) that

$$\sigma_\Theta(t)-\sigma_R(t)=\mu\left\{\eta_0\left[\left(\frac{f(t)}{R}\right)^2-\left(\frac{R}{f(t)}\right)^4\right]+\sum_{m=1}^{M}\eta_m\left[(\eta_m(t)+Y_{m,-2}(t))\left(\frac{f(t)}{R}\right)^2-(n_m(t)+Y_{m,4}(t))\left(\frac{R}{f(t)}\right)^4\right]\right\}. \tag{85}$$

In the absence of body forces, the equilibrium equation reads

$$\frac{\partial\sigma_R}{\partial r}+\frac{2}{r}(\sigma_R-\sigma_\Theta)=0. \tag{86}$$

We integrate eqn (86) from $r_1=f(t,R_1)$ to $r_2=f(t,R_2)$ and use the boundary conditions

$$\sigma_R(t,r_1(t))=-p(t),\quad \sigma_R(t,r_2(t))=0. \tag{87}$$

As a result, we obtain

$$p = 2\int_{r_1}^{r_2} (\sigma_\Theta - \sigma_R) r^{-1}\, dr.$$

We return to the variable R in the integrand with the use of eqns (75) and (80), substitute expression (85) into the obtained expression, and arrive at the nonlinear integral equation for the function $C(t)$

$$p(t) = 2\mu \int_{R_1}^{R_2} \left\{ \eta_0 \left[\left(1 + \frac{C(t)}{R^3} \right)^2 - 1 \right] + \sum_{m=1}^{M} \eta_m \left[(n_m(t,R) + Y_{m,-2}(t,R)) \left(1 + \frac{C(t)}{R^3} \right)^2 \right. \right.$$
$$\left. \left. - (n_m(t,R) + Y_{m,4}(t,R)) \right] \right\} \frac{R^6 dR}{(R^3 + C(t))^{7/3}}. \quad (88)$$

It follows from eqns (19) and (84) that the functions $n_m(t,R)$ and $Y_{m,k}(t,R)$ obey the ordinary differential equations (R is treated as a parameter)

$$\frac{\partial n_m}{\partial t}(t,R) = -\gamma_m(t,R) n_m(t,R), \quad n_m(0,R) = 1,$$
$$\frac{\partial Y_{m,k}}{\partial t}(t,R) = (\gamma_m(t,R)) \left[\left(1 + \frac{C(t)}{R^3} \right)^{k/3} - Y_{m,k}(t,R) \right], \quad Y_{m,k}(0,R) = 0. \quad (89)$$

The rates of reformation for adaptive links $\gamma_m(t,R)$ are governed by eqn (27), where the strain energy density $\tilde{W}_0$ is determined by eqns (34), (48), and (81)

$$\tilde{W}_0(t,R) = \frac{\mu}{2} \left[2 \left(1 + \frac{C(t)}{R^3} \right)^{2/3} + \left(1 + \frac{C(t)}{R^3} \right)^{-4/3} - 3 \right]. \quad (90)$$

We introduce the dimensionless variables

$$Z_* = \left(\frac{R}{R_1} \right)^3, \quad t_* = \gamma_{10} t, \quad p_* = \frac{p}{2\mu}, \quad C_* = \frac{C}{R_1^3},$$

and present eqns (88) to (90) as follows (asterisks are omitted for simplicity):

$$p(t) = \frac{1}{3} \int_1^{(R_2/R_1)^3} \left\{ \eta_0 [(1 + C(t) Z^{-1})^2 - 1] + \sum_{m=1}^{M} \eta_m [(n_m(t,Z) + Y_{m,-2}(t,Z))(1 + C(t) Z^{-1})^2 \right.$$
$$\left. - (n_m(t,Z) + Y_{m,4}(t,Z))] \right\} (1 - C(t) Z^{-1})^{-7/3} Z^{-1}\, dZ, \quad (91)$$

$$\frac{\partial n_m}{\partial t}(t,Z) = -\frac{\gamma_{m0}}{\gamma_{10} a(t,Z)} n_m(t,Z), \quad n_m(0,Z) = 1,$$
$$\frac{\partial Y_{m,k}}{\partial t}(t,Z) = \frac{\gamma_{m0}}{\gamma_{10} a(t,Z)} [(1 + C(t) Z^{-1})^{k/3} - Y_{m,k}(t,Z)], \quad Y_{m,k}(0,Z) = 0, \quad (92)$$

$$\ln a(t,Z) = \beta \{ [1 + \beta_0 (2(1 + C(t) Z^{-1})^{2/3} + (1 + C(t) Z^{-1})^{-4/3} - 3)]^{-1} - 1 \}. \quad (93)$$

To solve eqns (91) to (93) numerically in the dimensionless time interval $[0, T]$, we introduce a time step δ and divide the interval $[0, T]$ by points $t_n = n\delta$ ($n = 0, 1, \ldots, N$). At $n = 0$, the functions n_m and $Y_{m,k}$ are known, and eqn (91) can be treated as a nonlinear

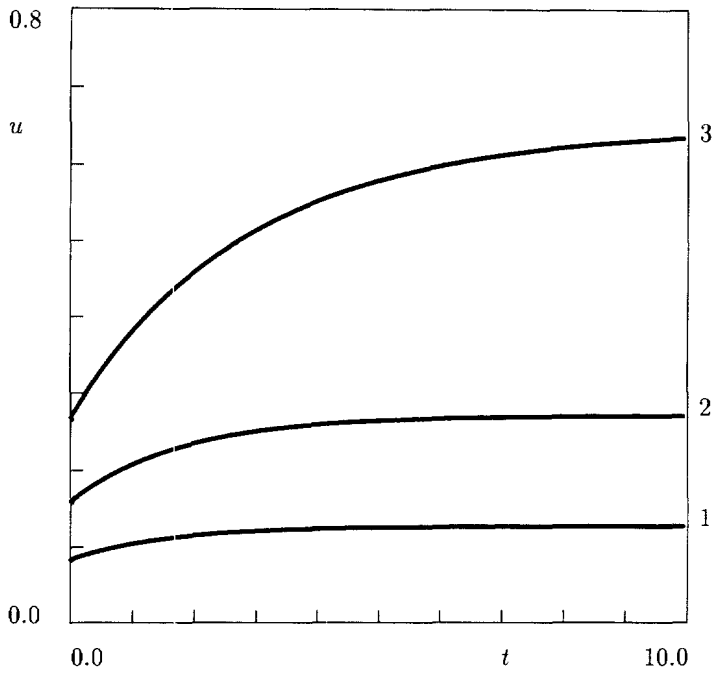

Fig. 15. The dimensionless displacement u of the inner surface vs the dimensionless time t for a nonlinear viscoelastic spherical vessel with $B = 1.0$ and $\beta = 0.1$. Curve 1, $p = 0.06$; curve 2, $p = 0.10$; curve 3, $p = 0.14$.

algebraic equation for C, which is solved by the bisection method. Using the obtained C value, we determine a from eqn (93). Afterwards we calculate the functions n_m and $Y_{m,k}$ at $n = 1$ by integrating eqn (92). Repeating the same procedure N times, we determine the function $C(t)$ for a given loading program $p(t)$. Using this function, we can easily calculate stresses and displacements in a spherical shell with the use of eqn (80) and (83). The radial displacement u on the internal surface of the vessel equals

$$u(t) = f(t, R_1) - R_1 = R_1[(1 + C(t))^{1/3} - 1].$$

The stress intensity S is determined as

$$S = \sqrt{\tfrac{3}{2}\mathbf{s} : \mathbf{s}},$$

where $\mathbf{s}$ is the deviatoric part of the Cauchy stress tensor $\boldsymbol{\sigma}$. For radial deformation of a sphere under the action of internal pressure.

$$S = \sigma_\Theta - \sigma_R.$$

Combining this equality with eqn (85), we arrive at the formula

$$S(t, Z) = \mu \left\{ \eta_0 \left[\left(1 + \frac{C(t)}{Z}\right)^{2/3} - \left(1 + \frac{C(t)}{Z}\right)^{-4/3} \right] \right.$$
$$\left. + \sum_{m=1}^{M} \eta_m \left[(n_m(t, Z) + Y_{m,-2}(t, Z)) \left(1 + \frac{C(t)}{Z}\right)^{2/3} - (n_m(t, Z) + Y_{m,4}(t, Z)) \left(1 + \frac{C(t)}{Z}\right)^{-4/3} \right] \right\}$$

Results of numerical simulation at $T = 10$, $R_2/R_1 = 1.4$, $M = 1$, and $\eta_0 = 0.7$ for a time-independent pressure $p =$ constant are presented in Figs 15–18, where the dimensionless displacement $u_* = u/R_1$ and the dimensionless stress intensity $S_* = S/\mu$ are plotted vs the

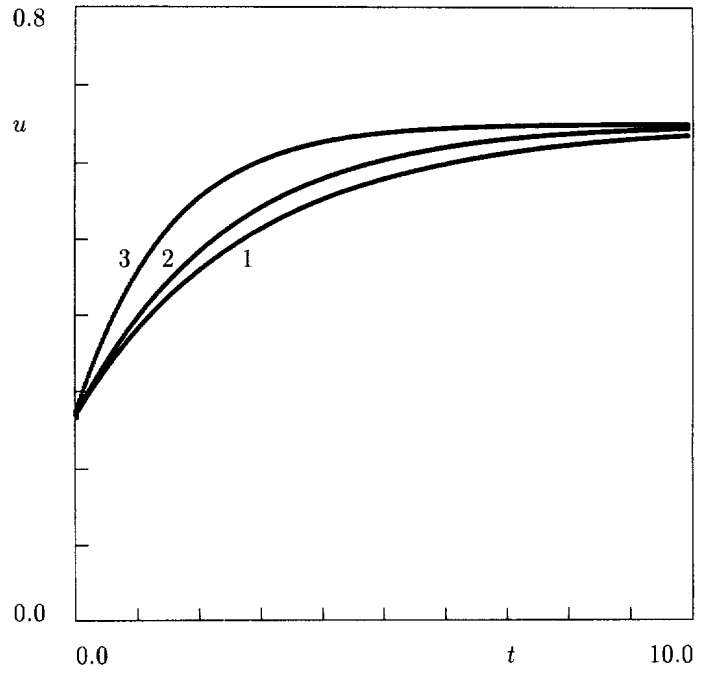

Fig. 16. The dimensionless displacement u of the inner surface vs the dimensionless time t for a nonlinear viscoelastic spherical vessel with $B = 1.0$ and $p = 0.14$. Curve 1, $\beta = 0.1$; curve 2, $\beta = 1.0$; curve 3, $\beta = 10.0$.

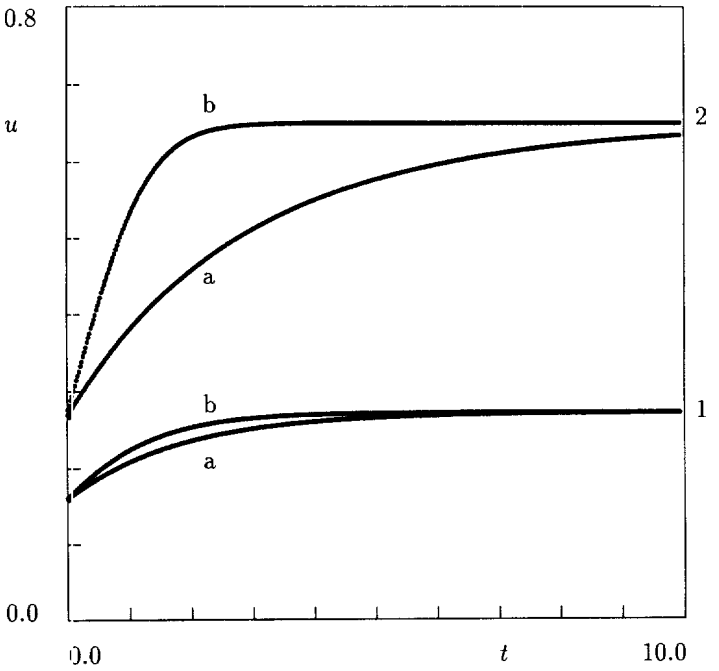

Fig. 17. The dimensionless displacement u of the inner surface vs the dimensionless time t for a nonlinear viscoelastic spherical vessel with $\beta = 0.5$. Curved 1, $p = 0.10$; curve 2, $p = 0.14$. Curve (a), $B = 0.1$; curve (b), $B = 10.0$.

dimensionless time t_* (asterisks are omitted for simplicity). The following conclusions are drawn:

(i) the creep process in a spherical pressure vessel is extremely nonlinear: for small loads, an increase in the radial displacement u is rather small, and the limiting displacement

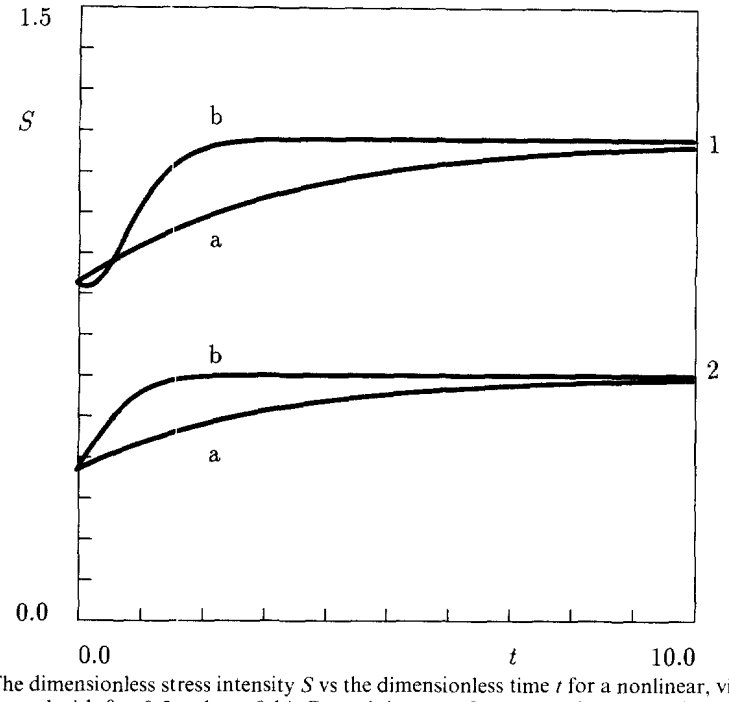

Fig. 18. The dimensionless stress intensity S vs the dimensionless time t for a nonlinear, viscoelastic spherical vessel with $\beta = 0.5$ and $p = 0.14$. Curve 1, inner surface; curve 2, outer surface. Curve (a), $B = 0.1$; curve (b), $B = 10.0$.

is reached relatively rapidly; for large pressures, the growth of the radial displacement is large, and significant time is necessary for the displacement to reach its limiting value, see Fig. 15;

(ii) the growth of the β value leads to an increase in the rate of creep and to a decrease in the time necessary to reach the limiting values of displacements. However, the effect of β on the radial displacement is rather weak: an increase in β by two orders of magnitude leads to an increase in u which does not exceed 30 per cent, see Fig. 16;

(iii) an increase in the B value affects stresses and displacements in a spherical vessel. The influence of B is rather strong for large pressures, and it becomes less pronounced for small loads. The growth of B entails an increase in the rate of creep, see Fig. 17, and an increase in the stress intensity, see Fig. 18;

(iv) for the standard K-BKZ constitutive equations with stress/strain independent relaxation spectra, the correspondence principle (the Alfrey theorem) is satisfied. According to it, stresses in a viscoelastic medium loaded by time-independent forces on the entire boundary surface are time-independent, since they are determined from an appropriate "elastic" problem. Figure 18 demonstrates that the correspondence principle is not valid for viscoelastic media with strain-dependent relaxation spectra. The stress intensities S on the inner and outer surfaces of the vessel increase in time and tend to some limiting values. The growth of stresses on the outer surface depends monotonically on B, while a non-monotonic dependence is observed on the inner surface (at the initial stage of loading). This phenomenon may be explained by inhomogeneity of stresses in the vessel, where large gradients of stresses arise in the vicinity of the inner boundary.

8. CONCLUDING REMARKS

New constitutive equations for the nonlinear behavior of viscoelastic media at finite strains are derived and verified by comparison of results of numerical simulation with experimental data (in tensile and shear tests) for a number of polymers. The model deals with viscoelastic materials which do not possess the separability property.

The constitutive model generalizes the concept of transient networks by assuming the rates of reformation and breakage for adaptive links to depend strictly on a strain energy density. A new phenomenological equation is proposed for the effect of strains on the shift factor, see eqn (23), which extends the Doolittle formula to viscoelastic media with mechanically induced relaxation spectra.

The model with a relatively small number M of different kinds of adaptive links ensures fair agreement with experimental relaxation curves, see Figs 1, 8, 10, and 14, and correctly predicts the material response in tensile tests with a constant rate of strains without any additional fitting adjustable parameters, see Fig. 7.

An important advantage of the model is that it can adequately describe the stress–strain dependencies with a local maximum (the yield-like behavior) and two local maxima (double yield) on the nominal stress–nominal strain curves. Analysis of experimental data for semicrystalline polymers leads us to a hypothesis that a high level of crystallinity may cause deviations from the separability property.

To demonstrate the influence of the strain inhomogeneity on stresses in a viscoelastic medium, we consider radial deformation of a thick-walled spherical pressure vessel. An explicit solution is derived, where the only function $C(t)$ is determined numerically by solving integro-differential eqns (91) through (93). It is shown that the correspondence principle is not valid for the model under consideration, and stresses change significantly in time even under the action of a time-independent internal pressure.

REFERENCES

Arutyunyan, N. K., Drozdov, A. D. and Naumov, V. E. (1987) *Mechanics of Growing Viscoelastoplastic Solids*, Nauka, Moscow [in Russian].

Bernstein, B. and Shokoch, A. (1980) The stress function in viscoelasticity. *Journal of Rheology* **24,** 189–211.

Bloch, R., Chang, W. V. and Tschoegl, N. W. (1978) The behavior of rubberlike materials in moderately large deformations. *Journal of Rheology* **22,** 1–32.

Brooks, N. W. J., Duckett, R. A. and Ward, I. M. (1992) Investigation into double yield points in polyethylene. *Polymer* **33,** 1872–1880.

Brooks, N. W. J., Duckett, R. A. and Ward, I. M. (1995) Modeling of double yield points in polyethylene: temperature and strain-rate dependence. *Journal of Rheology* **39,** 425–437.

Buckley, C. P. and Jones, D. C. (1995) Glass-rubber constitutive model for amorphous polymers near the glass transition. *Polymer*, **36,** 3301–3312.

Chengalva, M. K., Kenner, V. H. and Popelar, C. H. (1995) An evaluation of a free volume representation for viscoelastic properties. *International Journal of Solids and Structures* **32,** 847–856.

Doolittle, A. K. (1951) Studies in Newtonian flow. 2. The dependence of the viscosity of liquid on free-space. *Journal of Applied Physics* **22,** 1471–1475.

Drozdov, A. D. (1993) On constitutive laws for ageing viscoelastic materials at finite strains. *European Journal of Mechanics A/Solids* **12,** 305–324.

Drozdov, A. D. (1996) *Finite Elasticity and Viscoelasticity*, World Scientific, Singapore.

Drozdov, A. D. (1997) A constitutive model for nonlinear viscoelastic media. *International Journal of Solids and Structures* **34,** 2685–2707.

Ferry, J. D. (1980) *Viscoelastic Properties of Polymers*, Wiley, New York.

Glucklich, J. and Landel, R. F. (1977) Strain energy function of styrene butadiene rubber and the effect of temperature. *Journal of Polymer Science: Polymer Physics Edition* **15,** 2185–2199.

Green, M. S. and Tobolsky, A. V. (1946) A new approach to the theory of relaxing polymeric media. *Journal of Chemical Physics* **14,** 80–92.

Hasan, O. A., Boyce, M. C., Li, X. S. and Berko, S. (1993) An investigation of the yield and postyield behavior and corresponding structure of poly(methyl methacrylate). *Journal of Polymer Science: Polymer Physics Edition* **31,** 185–197.

He, Z. R. and Song, M. S. (1993) Elastic behaviors of swollen multiphase networks of SBS and SIS block copolymers. *Rheologica Acta* **32,** 254–262.

Isono, Y. and Ferry, J. D. (1985) Stress relaxation and differential dynamic modulus of polyisobutylene in large shearing deformations. *Journal of Rheology* **29,** 273–280.

Kaye, A. (1966) An equation of state for non-Newtonian fluids. *British Journal of Applied Physics* **17,** 803–806.

Khan, S. A., Prud'homme, R. K. and Larson, R. G. (1987) Comparison of the rheology of polymer melts in shear, and biaxial and uniaxial extensions. *Rheology Acta* **26,** 144–151.

Knauss, W. G. and Emri, I. J. (1981) Non-linear viscoelasticity based on free volume consideration. *Computers and Structures* **13,** 123–128.

Knauss, W. G. and Emri, I. J. (1987) Volume change and the nonlinearly thermoviscoelastic constitution of polymers. *Polymer Engineering and Science* **27,** 86–100.

La Mantia, F. P. (1977) Non linear viscoelasticity of polymeric liquids interpreted by means of a stress dependence of free volume. *Rheologica Acta* **16,** 302–308.

La Mantia, F. P. and Titomanlio, G. (1979) Testing of a constitutive equation with free volume dependent relaxation spectrum. *Rheologica Acta* **18,** 469–477.

Laun, H. M. (1978) Description of the non-linear shear behavior of a low density polyethylene melt by means of an experimentally determined strain dependent memory function. *Rheologica Acta* **17,** 1–15.
Leaderman, H. (1943) *Elastic and Creep Properties of Filamentous Materials*, Textile Foundation, Washington, D.C.
Litt, M. H. and Torp, S. (1973) Strain and temperature dependence of relaxation phenomena in polycarbonate. *Journal of Applied Physics* **44,** 4282–4287.
Lodge, A. S. (1968) Constitutive equations from molecular network theories for polymer solutions. *Rheologica Acta* **7,** 379–392.
Losi, G. U. and Knauss, W. G. (1992) Free volume theory and nonlinear thermoviscosity. *Polymer Engineering and Science* **32,** 542–557.
Lucas, J. C., Failla, M. D., Smith, F. L., Mandelkern, L. and Peacock, A. J. (1995) The double yield in the tensile deformation of the polyethylenes. *Polymer Engineering and Science* **35,** 1117–1123.
Marrucci, G. and de Cindio, B. (1980) The stress relaxation of molten PMMA at large deformations and its theoretical interpretation. *Rheologica Acta* **19,** 68–75.
McCrum, N. G. (1984) The kinetics of the α relaxation in an amorphous polymer at temperatures close to the glass transition. *Polymer* **25,** 309–317.
McKenna, G. B. and Zapas, L. J. (1979) Nonlinear viscoelastic behavior of poly(methyl methacrylate) in torsion. *Journal of Rheology* **23,** 151–166.
Muramatsu, S. and Lando, J. B. (1995) Double yield points in poly(tetramethylene terephthalate) and its copolymers under tensile loading *Polymer Engineering and Science* **35,** 1077–1085.
Petruccione, F. and Biller, P. (1988) Rheological properties of network models with configuration-dependent creation and loss rates. *Rheologica Acta* **27,** 557–560.
Read, B. E. (1981) Influence of stress state and temperature on secondary relaxations in polymeric glasses. *Polymer* **22,** 1580–1586.
Ricco, T. and Smith, T. L. (1985) Rejuvenation and physical ageing of a polycarbonate film subjected to finite tensile strains. *Polymer* **26,** 1979–1984.
Salem, D. R. (1992) Development of crystalline order during hot drawing of poly(ethylene terephthalate) film: influence of strain rate. *Polymer* **33,** 3182–3188.
Santore, M. M., Duran, R. S. and McKenna, G. B. (1991) Volume recovery in epoxy glasses subjected to torsional deformations: the question of rejuvenation. *Polymer* **32,** 2377–2381.
Schapery, R. A. (1966) An engineering theory of nonlinear viscoelasticity with applications. *International Journal of Solids and Structures* **2,** 407–425.
Seguela, R. and Rietsch, F. (1990) Double yield points in polyethylene under tensile loading. *Journal of Material Science Letters* **9,** 46–47.
Shay, R. M. and Caruthers, J. M. (1986) A new viscoelastic constitutive equation for predicting yield in amorphous solid polymers. *Journal of Rheology* **30,** 781–827.
Soskey, P. R. and Winter, H. H. (1985) Equibiaxial extension of two polymer melts: polystyrene and low density polyethylene. *Journal of Rheology* **29,** 493–517.
Struik, L. C. E. (1978) *Physical Ageing in Amorphous Polymers and Other Materials*, Elsevier, Amsterdam.
Tanaka, F. and Edwards, S. F. (1992) Viscoelastic properties of physically cross-linked networks. Transient network theory. *Macromolecules* **25,** 1516–1523.
Tervoort, T. A., Klompen, E. T. J. and Govaert, L. E. (1996) A multi-mode approach to finite, three-dimensional, nonlinear viscoelastic behavior of polymer glasses. *Journal of Rheology* **40,** 779–797.
Titomanlio, G., Spadaro, G. and La Mantia, F. P. (1980) Stress relaxation of a polyisobutylene under large strains. *Rheologica Acta* **19,** 477–481.
Tobolsky, A. V. and Eyring, H. (1943) Mechanical properties of polymeric materials. *Journal of Chemical Physics* **11,** 125–134.
Truesdell, C. (1975) *A First Course in Rational Continuum Mechanics*, Academic Press, New York.
Truss, R. W., Clarke, P. L., Duckett, R. A. and Ward, I. M. (1984) The dependence of yield behavior on temperature, pressure and strain rate for linear polyethylenes of different molecular weight and morphology. *Journal of Polymer Science: Polymer Physics Edition* **22,** 191–209.
Wagner, M. H. (1976) Analysis of time-dependent non-linear stress-growth data for shear and elongation flow of a low-density branched polyethylene melt. *Rheologica Acta* **15,** 136–142.
Waldron, W. K., McKenna, G. B. and Santore, M. M. (1995) The nonlinear viscoelastic response and apparent rejuvenation of an epoxy glass. *Journal of Rheology* **39,** 471–497.
Wilding, M. A. and Ward, I. M. (1981) Creep and recovery of ultra high modulus polyethylene. *Polymer* **22,** 870–876.
Wineman, A. S. and Waldron, W. K. (1993) Interaction of nonhomogeneous shear, nonlinear viscoelasticity, and yield of a solid polymer. *Polymer Engineering and Science* **33,** 1217–1228.
Wineman, A. S. and Waldron, W. K. (1995) Yieldlike response of a compressible nonlinear viscoelastic solid. *Journal of Rheology* **39,** 401–423.
Yamamoto, M. (1956) The visco-elastic properties of network structure. 1. General formalism. *Journal of the Physics Society of Japan* **11,** 413–421.
Yee, A. F., Bankert, R. J., Ngai, N. L. and Rendell, R. W. (1988) Strain and temperature accelerated relaxation in polycarbonate. *Journal of Polymer Science: Polymer Physics Editions* **26,** 2463–2483.